Hyperinsulinemic euglycemic clamp in anesthetized rat: A protocol for rat *in vivo* FDG PET studies

Anna Jalo

Turun yliopisto
University of Turku

Master´s thesis

University of Turku

Department of Biomedicine

Master´s degree in Biomedical Imaging

Supervisors: PhD Jarna Hannukainen (PI)

PhD Jatta Helin

ABSTRACT

UNIVERSITY OF TURKU
Department of Biomedicine, Faculty of Medicine

JALO, ANNA: Hyperinsulinemic euglycemic clamp in anesthetized rat: A protocol for rat in vivo FDG PET studies
Master's Thesis, 49 p
MSc Degree in Biomedical Imaging
August 2021

Obesity and physical inactivity are major public health issues in the population of the western countries. These conditions increase the risk for the development of insulin resistance and type 2 diabetes mellitus and lead to other complications, such as cardiovascular diseases, diabetic retinopathy, nephropathy, and neuropathy.

The "gold standard" for measuring tissue specific insulin sensitivity *in vivo* is to measure tissue glucose uptake using medical imaging modality positron emission tomography (PET) combined with the hyperinsulinemic euglycemic clamp. In this procedure insulin is administered to cause hyperinsulinemia while variable glucose concentration is administered to maintain euglycemia. Using radio-labeled glucose analogue tracer 2-deoxy-2-[18F]fluoro-D-glucose ([^{18}F]FDG) the amount of glucose taken up by specific tissues can be determined using PET. Even though the clamp method was adapted to preclinical studies with rats already in 1983, the preclinical method lacks universal guidelines and is subject to variations specific to the laboratory conducting the study.

The aim of this study was to establish a protocol for the Sprague Dawley laboratory rat strain for the hyperinsulinemic euglycemic clamp in combination with [^{18}F]FDG PET imaging. Different insulin infusion rates were compared to define the optimum conditions for the clamp and the set up for combining the insulin clamp with PET imaging was created.

Of the tested insulin infusion conditions, the two-stepped priming with 120 mU/kg/min for 2 minutes and 60 mU/kg/min for 2 minutes, followed by continuous infusion of 12 mU/kg/min produced the shortest time to reach and maintain euglycemia. A shunt system was created to accommodate for an automated blood sampling system to measure online *in vivo* blood radioactivity during the PET imaging.

This work describes a basic clamp protocol that can be adjusted for more rat strains and other species of laboratory animals. The shunt system can be used for dynamic PET studies generally to provide an arterial input function without the need to draw blood from the animal.

keywords: insulin resistance, hyperinsulinemic euglycemic clamp, microsurgery, rat, PET

TIIVISTELMÄ

UNIVERSITY OF TURKU
Biolääketieteen laitos, Lääketieteellinen tiedekunta

JALO, ANNA: Hyperinsulineeminen euglykeeminen clamp -tutkimus nukutetulle rotalle: Protokolla FDG-PET -tutkimuksiin
Pro Gradu -tutkielma, 49 s
MSc Degree in Biomedical Imaging
Elokuu 2021

Liikalihavuus ja fyysinen liikkumattomuus ovat suuri kansanterveydellinen ongelma länsimaiden väestössä. Nämä lisäävät insuliiniresistenssin sekä tyypin 2 diabeteksen riskiä ja voivat johtaa muihin komplikaatioihin, kuten sydän- ja verisuonitauteihin ja diabeteksen liitännäissairauksiin.

Kudoskohtaisen insuliiniherkkyyden määrittämisen parhaana standardimenetelmänä pidetään insuliini-clamp-tutkimusta yhdistettynä radiolääketieteelliseen kerroskuvausmenetelmään eli positroniemissiotomografiaan (PET). Tässä menetelmässä annostellaan tutkittavaan insuliinia hyperinsulinemian aikaansaamiseksi samalla, kun glukoosi-infuusiolla pidetään verensokeri tasaisena euglykeemisellä alueella. Kudoskohtaista glukoosin käyttöä voidaan mitata radioaktiivisilla isotoopeilla leimatuilla sokerijohdannaisilla yhdistettynä PET-menetelmään. Vaikka tämä menetelmä otettiin käyttöön prekliinisessä koe-eläintutkimuksessa jo vuonna 1983, ei vakiintunutta tutkimusmenetelmää ole määritetty kuten kliinisissä potilastutkimuksissa.

Tämän tutkimuksen tavoitteena oli luoda standardoitu tutkimusmenetelmä insuliini-clamp-tutkimukseen rotalle. Tutkimuksessa vertailtiin erilaisia insuliinin infuusiomääriä optimaalisen antomäärän määrittämiseksi. Tutkimuksessa selvitettiin mahdollisimman tehokas infuusiomäärä, jotta euglykeeminen tila saavutettaisiin mahdollisimman nopeasti.

Testatuista insuliininantomääristä kaksivaiheinen ”priming”, jossa annettiin insuliinia ensin 2 minuuttia 120 mU/kg/min infuusionopeudella ja seuraavaksi 2 minuuttia 60 mU/kg/min infuusionopeudella ennen ylläpitotasolle laskua (12 mU/kg/min), tuotti nopeimman tavan saavuttaa verensokerin euglykeeminen tasapainotila. Tutkimuksen osana luotiin myös tarvittava letkusto, jotta verta voidaan kierrättää kehon ulkopuolella automaattisen veren radioaktiivisuusmittarin läpi ilman verenhukkaa.

Tässä työssä kuvaillaan clamp-protokolla, jota voidaan tarpeen mukaan muokata käytettäväksi useampien rottakantojen tai muiden laboratorioeläinlajien kanssa. Veren radioaktiivisuuden mittaamista automaattisella mittarilla voidaan hyödyntää myös muissa kuin sokerianalogimerkkiainetutkimuksissa veren kineettisen mallintamisen määrittämiseksi.

avainsanat: insuliiniresistenssi, insuliini-clamp, mikrokirurgia, rotta, PET

List of used abbreviations

[^{18}F]FDG	2-Deoxy-2-[^{18}F]-fluoro-D-glucose
AIF	Arterial input function
Akt	Protein kinase B
DNA	Deoxyribonucleic acid
GIR	Glucose infusion rate
Grp2	growth factor receptor-bound protein 2
IRS1/2	Insulin receptor substrate 1 or 2
LC	Lumped constant
MAPK	Mitogen-activated protein kinase
MEK	Mitogen-activated protein kinase kinase
$MR_{glucose}$	Metabolic rate of glucose
mRNA	Messenger ribonucleic acid
PDK-1	3-phosphoinositide-dependent protein kinase-1
PET	positron emission tomography
PI3K	Phosphoinositide 3-kinase
PIP2	Phosphatidylinositol-4,5 diphosphate
PIP3	Phosphatidylinositol-3,4,5 triphosphate
PKC	Protein kinase C
ROI	Region of interest
SHC	SHC-transforming protein 1
SOS	Son of Sevenless
T2DM	Type 2 diabetes mellitus
TAC	Time activity curve

Table of Contents

1. Introduction

Obesity and physical inactivity are major public health issues in the population of the western countries. The prevalence of obesity has nearly tripled worldwide since 1975. In 2016, 39 % of adults were overweight and 13 % were obese. (WHO, 2020)

Obesity increases the risk for the development of insulin resistance and type 2 diabetes mellitus (T2DM). Like obesity, the incidence of T2DM is increasing at an alarming rate. In 2019 there were approximately 463 million people suffering from diabetes and it is estimated that the number will rise to 578 million by 2030 and to 700 million by 2040, increasing the prevalence by 51% and making it one of the fastest growing health challenges of the 21st century (International Diabetes Federation, 2019). T2DM is caused by impairment in the glucose metabolism, usually from insulin resistance. This chronic condition leads to hyperglycemia, which in turn can lead to other complications, such as cardiovascular disorders, diabetic retinopathy, nephropathy, and neuropathy (Muc et al., 2018). In addition to metabolic complications and diseases, impairment in insulin sensitivity has been shown to promote neurogenerative pathology and more than double the risk for Alzheimer's disease prevalence (Li, Leng and Song, 2015).

The "gold standard" for measuring whole body glucose uptake and insulin sensitivity has been the hyperinsulinemic euglycemic clamp since it was first introduced by DeFronzo et al. in 1979. In the method endogenous insulin secretion and hepatic glucose production are inhibited by exogenous insulin infusion and euglycemia is maintained by varying exogenous glucose infusion. The glucose infusion rate (GIR) needed to maintain euglycemia directly reflects insulin action. (DeFronzo, Tobin and Andres, 1979) The clamp method can even be used to study tissue specific glucose uptake by combining it with glucose analogue, 2-Deoxy-2-[^{18}F]-fluoro-D-glucose ([^{18}F]FDG), positron emission tomography (PET) studies. PET is a quantitative molecular imaging technique utilizing short-lived radioisotope-labelled tracers, to detect and measure biological processes *in vivo.* [^{18}F]FDG is a glucose analogue tracer that reflects the glucose metabolism until it phosphorylates into FDG-6-phosphate that can be imaged to define the amount of uptake.

The clamp protocol together with [^{18}F]FDG PET imaging is a highly demanding procedure, requiring trained staff and expensive equipment. Therefore, it is mainly used as a research tool to study the complex pathophysiology of insulin resistance rather than for diagnosing. Due to its rapidly increased prevalence, insulin resistance is widely studied and understood in humans together with insulin-mediated glucose metabolism, yet all the mechanism of the systems-level regulation of glucose homeostasis are not

known. Hence, preclinical animal studies can help by providing samples unattainable from humans *in vivo.*

The clamp method was adapted to preclinical studies with rats already in 1983 by Kraegen et al., but to this day lacks universal guidelines. Like the clinical protocol, the preclinical method requires skilled staff to perform the procedures. Preclinical clamping often requires microsurgery, and the small size and blood volume of study subject poses challenges for attaining all data necessary for quantitative kinetic analysis. This thesis focuses on developing a protocol for studying tissue specific glucose uptake *in vivo* in the Sprague Dawley laboratory rat strain, overcoming common challenges by introducing state-of-the-art technology for blood data collection.

2. Literature Review

2.1 Glucose homeostasis

Glucose is one of the main sources of energy for bodily functions, and especially important for the brain, as neurons are unable to efficiently use other substances as an energy source (Schönfeld and Reiser, 2013). It is therefore crucial for the body to ensure that there is always enough glucose circulating in the blood stream for the constant consumption by the brain, but at the same time control the level to protect the body from the harms caused by hyperglycemia. Circulating glucose is derived from three sources: intestinal absorption postprandially, glycogenolysis, and gluconeogenesis (Aronoff et al., 2004). The process of maintaining steady glucose level is called glucose homeostasis and is controlled by a complex neurohormonal system. The three main processes that must take place in a coordinated fashion after food intake are insulin secretion, followed by glucose uptake by tissues and suppression of hepatic glucose production. (DeFronzo, 1992)

Insulin is a hormone secreted from the β-cells of the pancreatic islets of Langerhans in increasing amount as a response to a rise in blood glucose level. Insulin works in a negative feedback loop together with glucagon to maintain glycemia. The effects are opposite with insulin decreasing the blood glucose by increasing glucose uptake into tissues to store as glycogen, whereas glucagon increases blood glucose concentration by endogenous glucose production, i.e. breaking glycogen down to glucose. After food intake the release of insulin occurs in two phases. There is an initial rapid release of preformed insulin, which is followed by increased synthesis and secretion of insulin in response to blood glucose concentration. If glucose remains high the result is long-term release of insulin. Insulin works in three main ways: firstly, by stimulating glucose uptake from the bloodstream into insulin-sensitive tissues, primarily striated muscle and adipose tissue; secondly it acts on the liver to promote glycogenesis, the storage of glucose as glycogen; thirdly by inhibiting hepatic glucose production in the liver by suppressing the levels of glucagon, which is a counteracting hormone to insulin controlling glycogenolysis and gluconeogenesis. (Aronoff et al., 2004)

The main site of glucose uptake in the postprandial state in humans is skeletal muscle (~80% of total glucose uptake). For glucose uptake and downstream processing to happen, insulin must bind to insulin receptors on the surface of the tissue cells, activating a cascade of protein phosphorylation-dephosphorylation reactions (PI3K-Akt signalling pathway). First, due to the binding on insulin onto the receptor, intracellular tyrosine residues auto-phosphorylate, leading to the phosphorylation of insulin receptor substrate

IRS1/2. This results in the binding of phosphatidylinositol (PI)-3 kinase to the IRS1/2 through the p85 regulatory subunit, activating the p110 catalytic subunit and leading to the phosphorylation of phosphatidylinositol-4,5 diphosphate (PIP2) to phosphatidylinositol-3,4,5 triphosphate (PIP3). The increase in the concentration of PIP3 recruits 3-phosphoinositide-dependent protein kinase-1 (PDK-1) to phosphorylate Akt (Protein kinase B), which in turn phosphorylates the Akt substrate 160 making it inactive. Inactivation of AS160 allows for the translocation of glucose transporter 4 containing vesicles to the cell surface, resulting in the transport of glucose inside the cell through the glucose transporter. Inside the cell, glucose is phosphorylated by hexokinase II and directed to oxidative or nonoxidative pathways. (DeFronzo and Tripathy, 2009)

In addition to glucose metabolism, insulin also influences lipid metabolism, attenuating fatty acid release from triglycerides in adipose tissue by inhibiting the hormone sensitive lipase and increasing lipid synthesis in adipose tissue and liver. Insulin increases amino acid transport into cells and diminishes lipolysis. It modulates transcription, affecting numerous mRNAs and thereby stimulates growth, DNA synthesis and cell replication (Ras-MAPK pathway). (Szablewski, 2011) The two main pathways are presented in Figure 1.

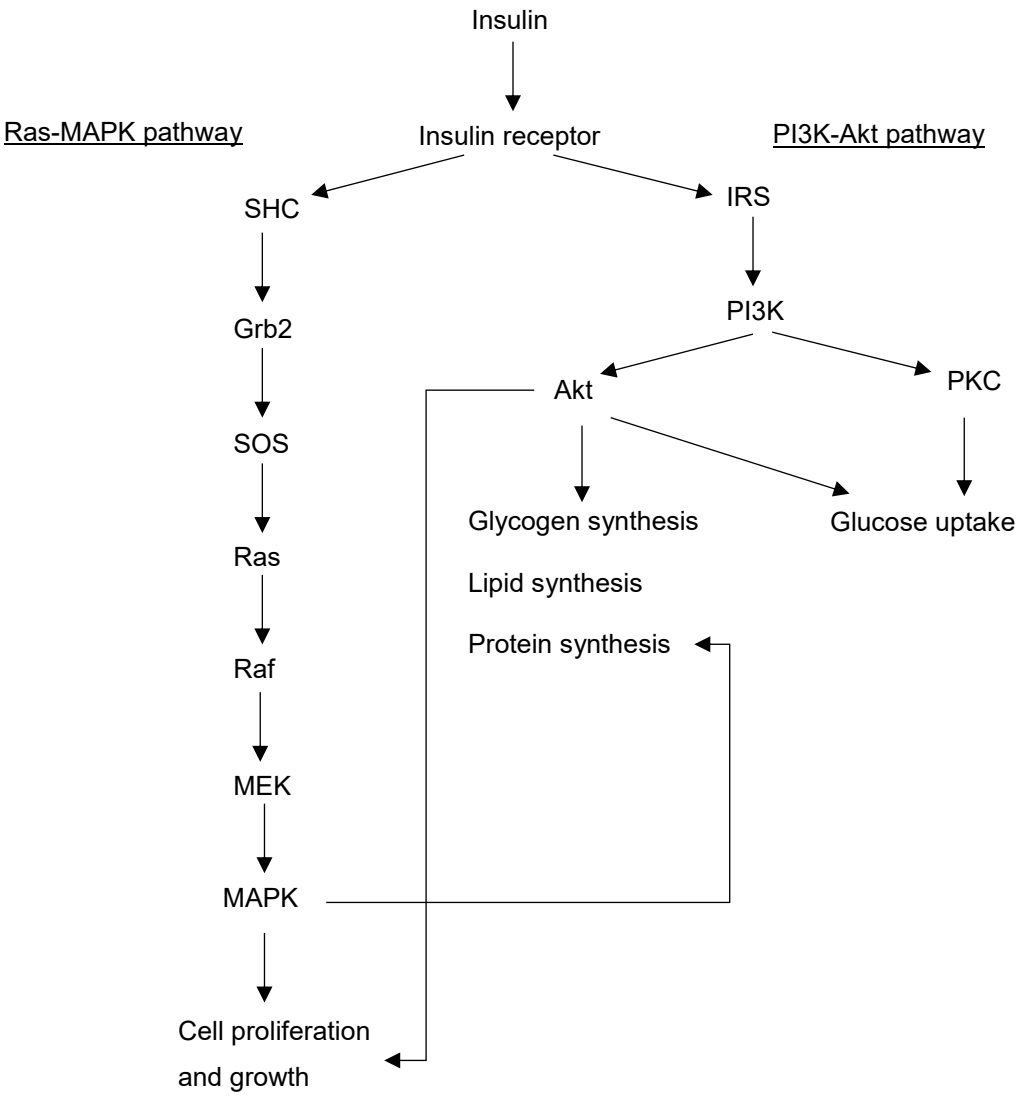

Figure 1 Simplified insulin signaling. cascades inside the cell. In the Ras-MAPK pathway the binding of insulin on the receptor causes adaptor proteins SHC-transforming protein 1 (SHC) and growth factor receptor-bound protein 2 (Grp2) to interact with the guanine nucleotide exchange factor Son of Sevenless (SOS), which in turn activates the guanosine-nucleotide-binding protein Ras. This leads to the activation of a protein kinase cascade. In the PI3K-Akt pathway the activation of insulin receptor leads to the phosphorylation of insulin receptor substrate (IRS). Phosphoinositide 3-kinase (PI3K) binds to IRS and phosphorylates phosphatidylinositol-4,5 diphosphate (PIP2) to phosphatidylinositol-3,4,5 triphosphate (PIP3). This recruits 3-phosphoinositide-dependent protein kinase-1 (PDK-1) to phosphorylate Protein kinase B (Akt) and Protein kinase C (PKC). *MAPK*, mitogen-activated protein kinase; *MEK*, mitogen-activated protein kinase kinase;

2.2 Insulin resistance

Insulin resistance is defined as attenuated biologic response in tissues to the hormone insulin. In insulin resistance, the body no longer effectively responds to the stimulus created by insulin and glucose uptake into tissues reduces. This means that cells have less glucose for energy metabolism, which leads to fatigue and desire for carbohydrates in attempt to gain more energy. This often leads to weight gain and increased adipose

tissue, which contributes to the insulin resistance by releasing inflammatory mediators and free fatty acids into the circulation. Increased level of fatty acids positively correlates with increased insulin resistance in the muscle. As the main site of glucose uptake in the postprandial state in humans is skeletal muscle, loss of insulin sensitivity in this tissue accounts greatly to insulin resistance. The reduced glucose uptake and elevated blood glucose concentration leads to increased release of pancreatic insulin in an attempt to compensate for the attenuated response, creating hyperinsulinemia. Over time, the pancreatic β-cells may get strained and can no longer keep up with the increased need for insulin. This eventually leads to partial or complete loss of function of the β-cells. When the body can no longer effectively lower blood glucose due to extreme insulin resistance or insulin resistance paired with impaired insulin production, the resulting state is hyperglycemia (Figure 2). (DeFronzo and Tripathy, 2009)

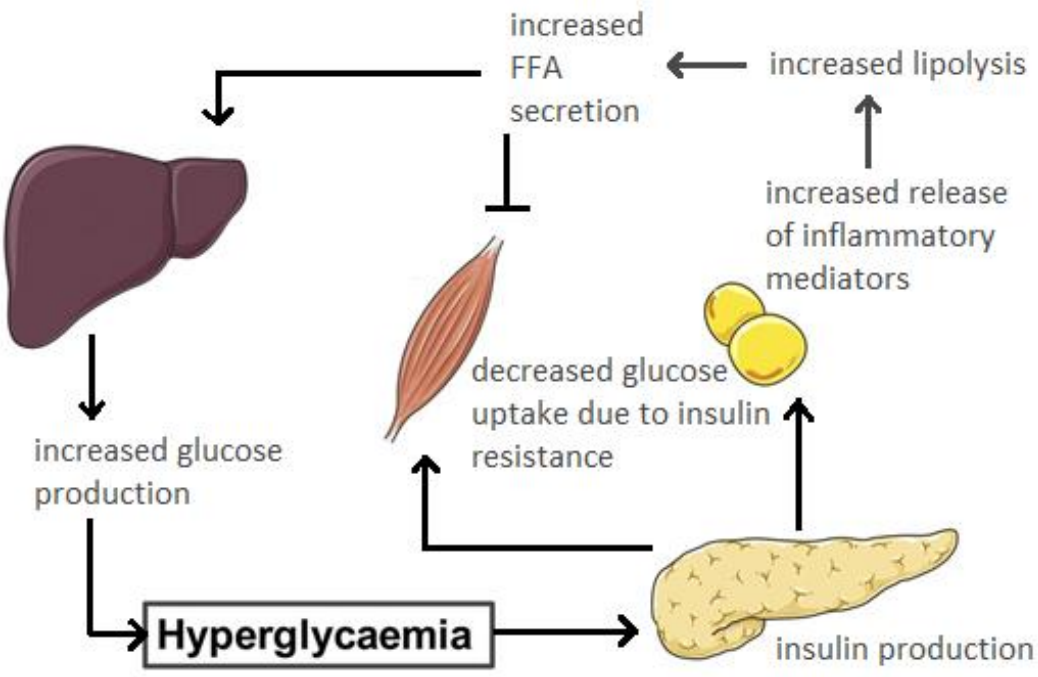

Figure 2 The simple mechanism of insulin resistance development and propagation. When the insulin-sensitive tissues develop resistance towards the action of insulin, glucose uptake into the tissues diminishes and the glucose remains in the blood flow. Insulin inhibition of inflammatory mediator release is attenuated, which leads to increased lipolysis and increased level of free fatty acids in the circulation. This further inhibits insulin action in the insulin-sensitive tissues. Inhibition of hepatic glucose production is also attenuated. Modified from Riddy et al., 2017.

2.2.1 Risk factors

Insulin resistance is often categorized as a lifestyle-disease. The typical “Western” diet high in sugar and saturated fatty acids, as well a sedentary lifestyle contributes greatly

to insulin resistance. As mentioned before, skeletal muscle is the main site of glucose uptake after a meal, so lack thereof diminishes the efficiency and rate of glucose uptake from the blood (Srikanthan and Karlamangla, 2011). Also, the two risk factors often lead to obesity, which strongly correlates with insulin resistance, as adipose tissue contributes to lipotoxicity.

Along with lifestyle-related risk factors, genetics play a role in the likelihood of developing insulin resistance. Insulin resistance is a highly heritable condition. The details of how for example T2DM, a disease caused by insulin resistance, is heritable are not yet known, but estimates range from 20 to 80 % based on different population, family, and twin-based studies (Poulsen et al., 1999; Meigs, Cupples and Wilson, 2000; Almgren et al., 2011). The lifetime risk for a first degree relative of a person with non-insulin dependent diabetes mellitus to develop diabetes is approximately 40 %, making them three times more likely to develop the condition than people with no family history (Perseghin et al., 1997; Florez, Hirschhorn and Altshuler, 2003). People with Mexican-Hispanic or African background tend to be more insulin resistant than Caucasian or East Asian descendants, East Asians being the most insulin sensitive of these groups (Golden et al., 2012; Kodama et al., 2013).

Based on previous research data women tend to have higher insulin-stimulated whole-body glucose disposal and uptake of glucose in skeletal muscle than men (Nuutila et al., 1995). Due to hormonal differences, the female body favors fat deposition in the glutes and thighs as opposed to abdominal deposition in males, which likely explains the difference in insulin sensitivity between the sexes (Hocking et al., 2013).

As people age, it is typical that physical activity decreases and metabolism slows, leading to loss of muscle mass and weight gain (Morley et al., 2013; Fuggle et al., 2017) which in turn increase the risk for insulin resistance. Smoking is also associated with high risk for developing insulin resistance (Haj Mouhamed et al., 2016).

2.4 Methods for assessing insulin sensitivity

2.4.1 Methods assessing whole body glucose uptake

Hyperinsulinemic euglycemic clamp

The hyperinsulinemic euglycemic clamp technique developed by DeFronzo et al. in 1979 is considered the golden standard technique of assessing whole body glucose uptake and insulin sensitivity in humans and is widely accepted as the reference standard method in clinical use. In this procedure, insulin is administered to cause

hyperinsulinemia while variable glucose concentration infusion is administered to maintain euglycemia. GIR needed to maintain euglycemia reflects the insulin action. (DeFronzo, Tobin and Andres, 1979)

The clamp is performed in a fasted state to exclude glucose uptake from the gastro-intestinal tract. A cannula is placed into the antecubital vein of a patient with ports for glucose and insulin infusion. The other arm is cannulated for blood sampling. The patient is awake but resting for the duration of the clamp procedure. The clamp is initiated by starting with the insulin infusion. The infusion rate can be constant throughout the study or primed with a higher concentration at the beginning. Due to the hyperinsulinemia, pancreatic insulin production and hepatic glucose production is inhibited (Wasserman et al., 2009.). This state would lead to hypoglycemia if the euglycemia was not maintained by introducing exogenous glucose. During clamp, blood glucose level is monitored at short intervals, usually 5 minutes, from a venous sample using a laboratory glucose analyzer or a portable glucometer if laboratory analysis is not feasible. Based on the blood glucose reading, glucose infusion is adjusted to maintain euglycemia, i.e. the plasma glucose level is “clamped” to a predefined target level, usually 5.0 mmol/L. When the hepatic glucose production is completely suppressed, the exogenous glucose infusion reflects total of the glucose uptake into the tissues i.e., the whole-body glucose disposal rate (Figure 3). The clamp is continued for a prolonged period of time to reliably define the average glucose infusion rate that is needed to maintain the target plasma glucose level with a certain constant insulin infusion. (DeFronzo, Tobin and Andres, 1979)

The whole-body glucose disposal rate (M-value) is a validated, common clinical outcome for estimating insulin sensitivity in diabetes-related studies. It is derived from the GIR and can be expressed in different ways, making it challenging to compare between studies. The glucose uptake is most often reported per body weight in kilograms or per fat-free mass. The use of fat-free mass is based on the major contribution of the muscle to the glucose uptake, making large fat mass understate the whole-body insulin sensitivity. However, large fat mass increases the contribution of adipose tissue in the glucose uptake (Dadson et al., 2015).

The GIR is dependent on the insulin infusion rate, and different cut-off values for corresponding insulin infusion rates have been defined to determine insulin resistance (Tam et al., 2012). Even when the hyperinsulinemic-euglycemic clamp has been the standard reference method for the past four decades, its laboriousness prevents it from being used as a standard procedure for diagnosing insulin resistance, but rather a valuable tool for research purposes.

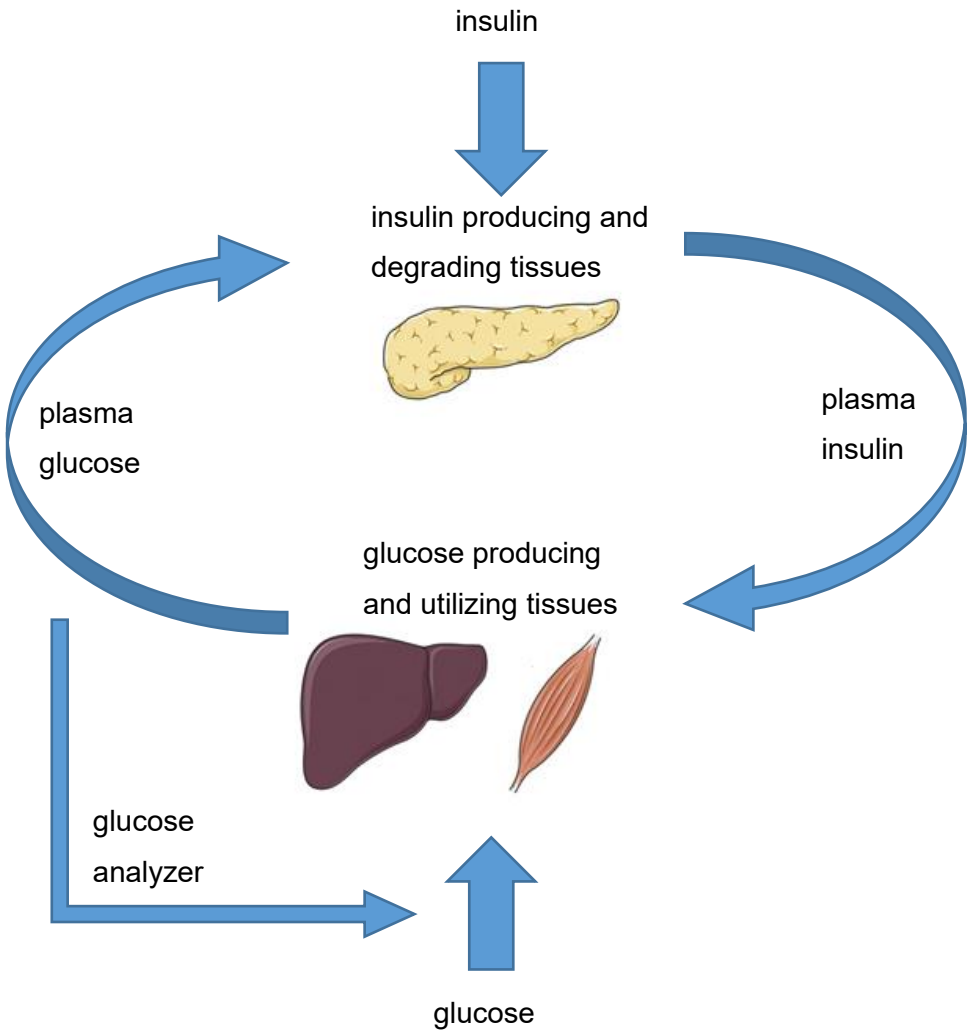

Figure 3 The principle of hyperinsulinemic euglycemic clamp during "steady state". Administered insulin and subsequent hyperinsulinemia suppresses endogenous insulin production. Fasting depletes glycogen storages, so the body relies on exogenous glucose to maintain plasma glucose level. When the plasma glucose level is stable, the glucose infusion rate reflects the uptake into glucose utilizing tissues. Modified from DeFronzo, 2015.

Even though the clamp method was adapted to preclinical studies with rats already in 1983 by Kraegen et al., the preclinical method lacks universal guidelines and is subject to variations specific to the laboratory conducting the study. The infused insulin conditions along with other variables vary significantly in the literature (Table 1). The main difference in clinical and preclinical study subject preparation for clamp is that rats need to be anesthetized for cannulation. The preclinical procedure is also more invasive, as the two main sites of cannulation, right jugular vein and right carotid artery or the femoral vein and artery, require surgical approach. Due to the invasive approach, many clamp experiments have been conducted under anesthesia (Spring-Robinson et al., 2009; Su et al., 2014; Lapa et al., 2017). With this approach no recovery time is needed

Table 1. Insulin clamp conditions of previous studies. Values are means±SE unless otherwise stated.

Laboratory	Rat strain	Sex	N	Age (wk)	Weight, g	Fasting period (h)	Anesthesia	Basal blood glucose mmol/L	Steady-state blood glucose mmol/L	Constant insulin infusion mU/kg/min	Steady state GIR mg/kg/min
Kraegen et al., 1983	Wistar	M	9	12	353±10	6 – 10	Conscious	4.2±0.1	4.2±0.1	1.67	10.6±0.6
James, Jenkins and Kraegen, 1985	Wistar	M	6	N/A	325-390*	5	Conscious	4.3±0.1	4.3±0.1	14	28.6±1.8
James, Jenkins and Kraegen, 1985	Wistar	M	6	N/A	325-390*	5	Conscious	4.0±0.1	4.0±0.1	2.4	13.4±1.4
Spring-Robinson et al., 2009	Sprague-Dawley	M	7	N/A	262±7**	14	Isoflurane	5.9±0.4**	5.9±0.5**	10	12.9±1.8**
Su et al., 2014	Sprague-Dawley	M	5	N/A	269.4±11.5**	overnight	Isoflurane	appr. 7	appr. 7.2***	5	12.6±1.6**
Lapa et al., 2017	Zucker diabetic fatty	M	6	13	356±24**	>10	Isoflurane	N/A	3.9-6.1***	12	N/A

Note: *Statistics not available; **Values are means±SD; ***only target value reported

Abbreviations: N, number of animals in the study group; GIR, glucose infusion rate; M, male

after the cannulation. The rat can also be chronically catheterized by placing the cannula where the animal does not have access to it, to allow the rat to be woken after the surgery and be conscious for the clamp (Kraegen et al., 1983). The animal should recover fully from the cannulation operation before initiating the clamp. The chronically catheterized conscious rat might be unrestrained or restrained during the clamp (Ayala et al., 2006).

One reason for the diversity of protocols used in the preclinical clamp with rats is the vast selection of different strains with varying characteristics. The most common strains used are Wistar and Sprague-Dawley (Kraegen et al., 1983; Spring-Robinson et al., 2009; Su et al., 2014) of the “common” strains and the Zucker diabetic fatty (Lapa et al., 2017) of the diabetes disease models. Males are used far more often (Spring-Robinson et al., 2009; Su et al., 2014; Lapa et al., 2017) than females, as females are almost exclusively used to study the effects of pregnancy on glucose homeostasis (Nieuwenhuizen et al., 1998; Einstein et al., 2008).

Oral glucose tolerance test

The oral glucose tolerance test (OGTT) is the standard test in clinical use for the diagnosis of glucose intolerance and T2DM due to minimal invasiveness and time consumption while providing more accurate results than surrogate measures. It is performed in a fasting state. A glucose load is given to the subject orally, after which plasma glucose is measured at predetermined points in time. The usual glucose load in clinical use for adults is 75 g and 2-h time point is used to diagnose impaired glucose tolerance T2DM. The threshold for diagnosis is fasting plasma glucose ≥126 mg/dL (7.0 mmol/L) or plasma glucose ≥200 mg/dL (11.1 mmol/L) 2 hours after the oral glucose load. (American Diabetes Association, 2015) If OGTT is used to measure insulin resistance, insulin levels need to be measured during the test along with plasma glucose since pancreatic insulin secretion is a major factor affecting the glucose levels. If the insulin secretion is impaired, high glucose levels might be measured without marked insulin resistance. Additional limitations to the accuracy of OGTT measurements are differences in gastric emptying between individuals, intestinal absorption as well as blood flow in the gastrointestinal organs (Hücking et al., 2008).

The principle for OGTT in rats is the same as in humans, but like the clamp, the conditions for the test vary. Differences in the length of the fasting period and glucose load make it difficult to compare between studies. The most common fasting period is overnight and the glucose load 2 grams per kilogram of body weight (Muniyappa et al., 2008). The length of the fasting period affects the basal hematological values (Kale et al., 2009) Oral gavage for administering the glucose load is stressful for the animal and

requires skill from the staff performing the procedure to prevent damage to the esophagus. The stress may be minimized by anesthetizing the animal for dosing. The weight-dependent dosing might also lead to misdiagnosing glucose intolerance: obese animals often gain weight is fat mass and might subsequently receive a bigger glucose for the same lean mass as lean animals. (Benedé-Ubieto et al., 2020)

Intravenous glucose tolerance test

The most common out of the various types of intravenous glucose tolerance tests (IVGTT) in clinical use is the frequently sampled intravenous glucose tolerance test (FSIVGTT). The test requires fasted state and begins by giving the subject a bolus of glucose intravenously over the period of 2 minutes. Plasma glucose and insulin samples are collected every few minutes for the first 30 minutes of the test and continued less frequently up until 180 minutes. An index for insulin sensitivity is computed using the plasma and insulin concentrations. (Bergman et al., 1979; Pacini and Bergman, 1986; Boston et al., 2003)

IVGTT is not very popular choice of method for glucose intolerance testing, as the route for dosing and frequent blood sampling brings discomfort for the experimental animal. The animal may be chronically catheterized for the experiment like for the clamp (Gauna et al., 2007), but the laboriousness does not correlate well with the usefulness of the test.

Fasting surrogate measures for assessing insulin sensitivity

Surrogate insulin sensitivity indices derived from fasting plasma glucose and insulin levels represent the simplest way in clinical use to assess insulin sensitivity. These include for example the Homeostatic model assessment for insulin resistance (HOMA-IR) (Matthews et al., 1985) and the Quantitative insulin sensitivity check index (QUICKI) (Katz et al., 2000). The indices were developed for humans and when tested with murine species, have shown only moderate correlation with GIR attained from clamp studies (Lee et al., 2008; Muniyappa et al., 2009).

2.4.2 Imaging tissue specific glucose uptake with positron emission tomography

The universal method for measuring tissue specific insulin stimulated glucose uptake *in vivo* is the hyperinsulinemic euglycemic clamp, or insulin clamp, combined with radioisotope-labelled glucose analogue and noninvasive positron emission tomography (PET). PET is a quantitative molecular imaging technique utilizing short-lived radioisotope-labelled molecules, i.e. tracers, to detect and measure biological processes *in vivo.* Radioactive isotopes, such as ^{11}C or ^{18}F, are produced in cyclotrons in the presence of a high-energy beam in a strong magnetic field, where a stable atomic

nucleus is bombarded with positively charged particles, creating a radioactive isotope with an extra proton. These isotopes decay by positron emission. In positron emission, the extra proton in the radioisotope nucleus is converted into a neutron while releasing a positron and an undetectable electron neutrino. After the tracer has been administrated into a study subject via intravenous or intraperitoneal route, the positron travels for only a short distance (less than 1 mm) before slowing down enough to interact with its antiparticle, electron, leading to annihilation. The collision of positron and electron annihilates the masses producing two 511 keV gamma photons traveling in opposite directions. The coincidental photon emission is detected by the scintillators of the detector rings in the PET imaging device and the spatial location where the photons originated can be determined (Figure 4). The data from coincident events is used to reconstruct a three-dimensional image, where signal intensity is directly proportional to the amount of tracer. The signal is corrected for scatter and the attenuation in the tissues through which it travels, using an anatomical reference image attained by computer tomography or magnetic resonance imaging. (Phelps, 2000; Saha, 2016)

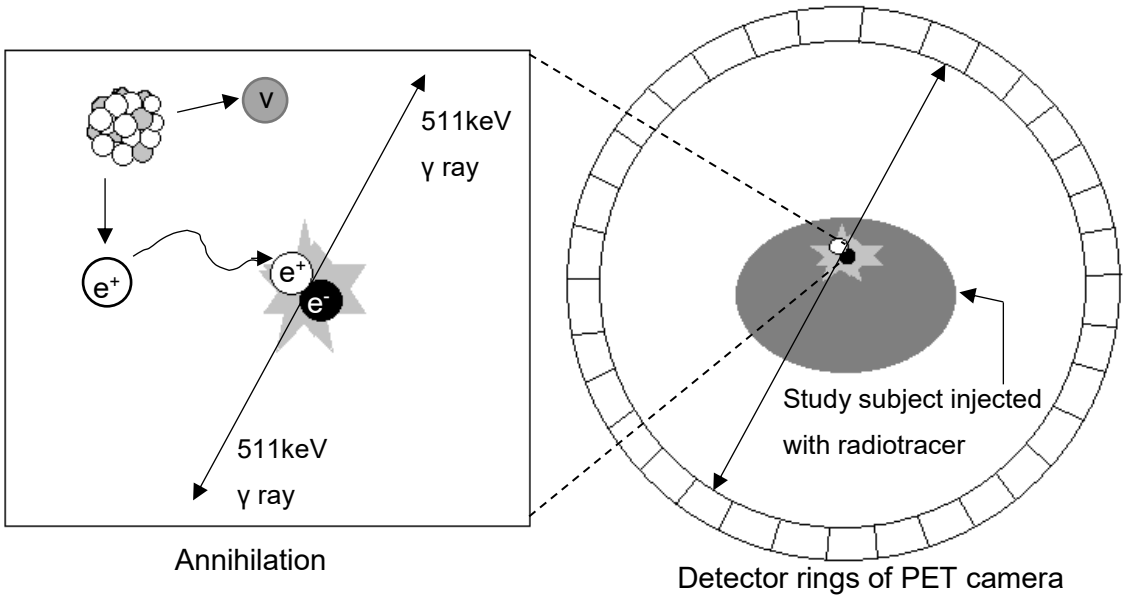

Figure 4 Basic principle of PET imaging. Radioactive tracer is introduced into the subject. The radionuclide decays via positron emission. The emitted positron travels until it loses enough kinetic energy to interact with an electron, causing annihilation. Two 511keV photons are released in nearly opposite directions as a result. The coincidental gamma rays are detected, and the data from the detected decay is used to reconstruct a 3D image of the radioactivity distribution.

Two main types of image acquisition protocols are used for PET scans: static and dynamic. A static scan is acquired after a certain period of time after the tracer injection to measure the distribution of the tracer. A static scan acquisition usually takes a few minutes. A dynamic scan is started at the time of injection and multiple image frames

are recorded to follow tracer distribution and uptake into tissues over time. The multiple radioactivity measurements are used to form time activity curves (TACs) for different regions of interest (ROI). (Braune et al., 2019)

[^{18}F]FDG is the only glucose analogue tracer available for *in vivo* use. It is derived from D-glucose and 2-Deoxy-D-glucose by labelling the second carbon atom of the cyclohexane structure with fluorine-18 instead of a hydroxyl group as in D-glucose, or hydrogen like in 2-Deoxy-D-glucose (Figure 5). [^{18}F]FDG has a favorable structure for glucose uptake measurement as it is transported into cells similarly as glucose, but has limited metabolism. After the initial uptake both glucose and [^{18}F]FDG are phosphorylated by hexokinase. Unlike glucose, [^{18}F]FDG is not further metabolized by glycolysis or glycogenesis, and its metabolism to the pentose phosphate pathway is very slow. Instead the phosphorylated [^{18}F]FDG is metabolized to radioactive metabolites and trapped intracellularly, where the radioactive signal can be detected. (Lin and Alavi, 2019)

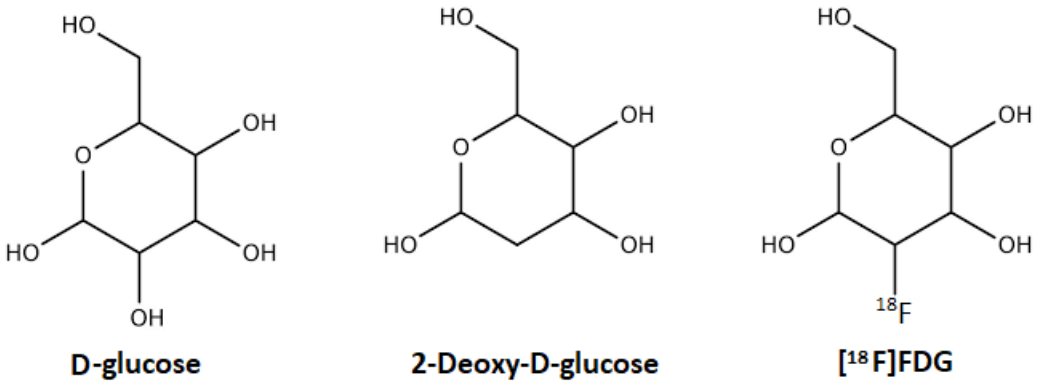

Figure 5 Molecular structures for D-glucose, 2-Deoxy-D-glucose and 2-Deoxy-2-^{18}F-fluoro-D-glucose ([^{18}F]FDG)

The [^{18}F]FDG-PET data can be analyzed using semi-quantitative methods or quantitative full kinetic modeling. Common simple semi-quantitative measurement of uptake in tissue is the standardized uptake value (SUV). SUV values are calculated by dividing the tissue radioactivity concentration at a given time by the injected dose and subject body weight. The pitfall of SUV is that it is affected by many factors, such as plasma glucose, patient weight and body composition, scanning time length and equipment calibration. (Keyes, 1995) Standardizing the scanning conditions can overcome most of these issues, but the SUV is still inferior when compared to quantitative kinetic modeling. Kinetic modeling requires dynamic PET acquisition as well as the arterial input function (AIF). AIF is derived from blood radioactivity, measured at various timepoints after injection. This requires repetitive blood sampling, which may bring discomfort to the study subject and

requires trained lab personnel and equipment for the measurements. If blood sampling is not feasible or successful, an estimate can be derived from the PET image. A state-of-the-art solution to avoid laborious sampling, but acquire better accuracy than image-derived method, is to use an automated blood sampling system that can measure the blood radioactivity in real time in a closed arteriovenous shunt. Swisstrace Twilite (Swisstrace GmbH) is an example of a commercially available coincidence detector for blood radioactivity measurement. Zhang et al. (2014) has proven that it can be used to assess AIF in clinical use, and it has also superior accuracy providing AIF in small rodents, when compared to image-derived input functions (Alf et al., 2012; MacAskill et al., 2019). The TACs and AIF are used to derive single rate constants describing forward membrane transport of FDG (K_1), backward membrane transport (k_2), phosphorylation of FDG (k_3) and dephophorylation of FDG (k_4) in a compartmental model (Figure 6) (Phelps et al., 1979).

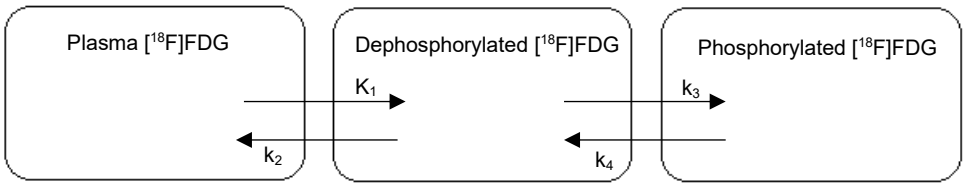

Figure 6 Standard two-tissue compartmental model used for ^{18}F-FDG kinetic modeling. K_1 is the rate of tracer across the membrane from plasma into tissue, k_2 is the rate of tracer across the membrane from the tissue to plasma, k_3 is the rate constant of tracer phosphorylation and k_4 the rate constant for dephosphorylation.

The uptake rate constant of [^{18}F]FDG (K_{FDG}) can be calculated from the following equation:

$$K_{FDG} = \frac{K_1 \times k_2}{k_2 + k_3} \qquad \text{(Equation 1)}$$

Dephosphorylation (k_4) is assumed to be 0. The metabolic rate of glucose ($MR_{glucose}$) is is estimated by dividing K_{FDG} by the lumped constant (LC), which corrects the difference of transfer rates between glucose and [^{18}F]FDG, and multiplying it with plasma glucose concentration ($C_{glucose}$):

$$MR_{glucose} = \frac{K_{FDG}}{LC} \times C_{glucose} \qquad \text{(Equation 2)}$$

Simplified, when [^{18}F]FDG is injected intravenously in conjunction with an insulin clamp, tissue specific glucose uptake can be measured, and metabolic rate defined. The insulin clamp reveals whole body glucose uptake rate, and the tracer uptake reveals how the glucose is distributed among different tissues. When this data is combined with measure of tracer concentration in the plasma over time, the delivery rate to tissues can be determined. (Ayala et al., 2006.)

Tissue specific glucose uptake with FDG-PET and hyperinsulinemic euglycemic clamp has been studied in rat models even in the recent years using mostly semi-quantitative analysing methods (Kaiser et al., 2013; Lapa et al., 2017) but results attained by kinetic modeling are still scarce (Nieuwenhuizen et al., 1998). This is probably due to the laboriousness of the technique and difficulty in attaining all the required data for a kinetic analysis. Yet preclinical research is crucial in the quest for mechanisms level understanding of insulin resistance, as clinical research cannot provide e.g. brain samples.

2.5 Physiological factors in *in vivo* PET clamp research practices

2.5.1 Blood circulation

The circulatory system of a laboratory rat is very similar to that of a human. The recommended mean for calculating total volume of blood in rats is 64 ml/kg, translating to approximately 6.5 % of the body weight in grams. The small and limited amount of blood may present challenges for blood sampling. With multiple sampling, meaning drawing very small amounts of blood multiple times within a short timeframe, the maximum blood sample volume removed can be up to 20 % of the total volume without significant disturbance to the normal physiology of the animal. With single sampling no more than 15 % of the total blood volume should be removed as this may result in hypovolemic shock. The recovery time after this kind of sampling is from three to four weeks. The capacity of the circulation also sets boundaries for intravenous infusions. The recommended maximum dose volume of discontinuous intravenous infusion for rat is 20 ml/kg and the maximum infusion rate 5 ml/kg/h. (Diehl et al., 2001)

2.5.2 Anesthesia and analgesia

As the insulin clamp is an invasive procedure requiring microsurgery to insert cannulas it is performed under anesthesia. Anesthesia is also required to keep the animals immobilized for the in vivo imaging of the radiotracer. Due to easy administration and adjusting over prolonged periods of time, isoflurane inhalation method is often applied. Previous study has shown that isoflurane inhibits insulin release by sarcolemmal

adenosine triphosphate -sensitive potassium channel activation, causing hyperglycemia (Tanaka et al., 2009; Zuurbier et al., 2008). However, other research also shows that even though isoflurane affects the basal secretion of insulin, is does not interfere with insulin sensitivity (Sano et al., 2016). Other effects of isoflurane include increased heart rate and mild hypotension (Albrecht et al., 2014). It decreases the [^{18}F]FDG uptake in brown fat and skeletal muscle, but increases the [^{18}F]FDG uptake in myocardium (Lømo et al., 2019).

Along with anesthesia, analgesia is needed to perform invasive surgery to relieve pain-induced stress, especially with isoflurane due to its poor analgesic properties (Cheng, Yeh and Flood, 2008). Buprenorphine is a long-acting opioid with both agonist and antagonist properties. It is used in post-operative care, treating chronic pain and opioid dependence. Due to its unique pharmacological profile, it has advantages over full opioid receptor agonists, such as morphine, fentanyl, codeine, and methadone. Very high affinity means it can replace other agonists and help overcome opioid dependence issues and slow dissociation from the receptor leads to prolonged therapeutic effect. It has significantly reduced adverse side effects compared full antagonists, but they are similar. Most common include nausea, vomiting, constipation, and respiratory depression. The latter has a ceiling effect and makes buprenorphine one of the safest opioids, but very careful consideration with dosing is recommended when combined with general anesthesia. (Khroyan et al., 2014; Lutfy and Cowan, 2004) Buprenorphine has also been shown to cause so called pica behavior in rats, meaning the consumption of non-nutrient substances such as bedding material, potentially leading to gastric distention. (Bosgraaf et al., 2004)

2.5.3 Temperature

Temperature is an important factor affecting biologic processes. Rat is a homeothermic mammal, aiming to keep their core body temperature steady. Changes in the ambient temperature will alter their metabolic rate as the main physiological response. The tail plays a key role in regulating body temperature. Vasodilation allows for heat loss and vasoconstriction reduces body heat loss through the tail. The animals also control the core temperature by adjusting the amount of behavioral thermoregulatory activity, such as increased movement, huddling or extension of limbs. (Suckow et al., 2019) In the absence of movement, i.e. when the animal is resting, sleeping or anesthetized, tonic motor unit causes isometric contractions and thus creates heat (Lømo et al., 2019).

Hypothermia reduces the metabolism of glucose, both endogenous and exogenously administered. It also prevents secretion of insulin and reduces the effectiveness of

administered insulin. Both these effects lead to hyperglycemia in hypothermic animals. (Fuhrman and Fuhrman, 1965; Steffen, 1988) Opposed to the effect of isoflurane, hypothermia increases [^{18}F]FDG uptake especially in brown fat and to some extent the skeletal muscle (Fueger et al., 2006).

2.5.4 Handling related stress

Multiple factors in the environment of laboratory rats may cause stress to the animal. Starting with indirect handling of the animal, the simple act of moving or transporting the cage results in elevated corticosterone levels in rodents. Another significant source of stress is noise in the study area. Loud and sudden noised understandably may startle the animal, but also softer and continuous noises such as humming of ventilation or sounds of machinery potentially induce stress in the animal (Armario, Montero and Balasch, 1986; Ravindran et al., 2005).

Direct handling of the animal by humans during husbandry or study procedures is always stressful for the animal. The level of stress may be subdued and controlled by regular handling of the animals by the same person, with similar frequencies of handling and standardized manner. (Dobrakovová et al., 1993)

3. Aim of the study

The overall aim of this thesis was to create a protocol for hyperinsulinemic euglycemic clamp for rats that could be used simultaneously with *in vivo* [^{18}F]FDG PET imaging. The following objectives were defined:

I. Compare different insulin infusion rates to define the optimum conditions for the hyperinsulinemic euglycemic clamp. The goal is to find the shortest time to achieve “steady state” in clamp to minimize the time the experimental animal is anesthetized. Worksheet templates are created to monitor different parameters of the protocol, such as glucose infusion rate and anesthesia.

II. Define the optimum shunt set-up for the future in vivo PET-imaging studies together with Swiss Trace II. The parameters under scrutiny are the shunt length, entry points and sample collection points.

4. Materials and methods

4.1 Study design

The study was carried out in three parts. Study timeline is presented in Figure 7. The three parts were not conducted in the chronological order of the timeline. Parts 1 and 2 were conducted in a laboratory setting without moving the animal to the PET camera.

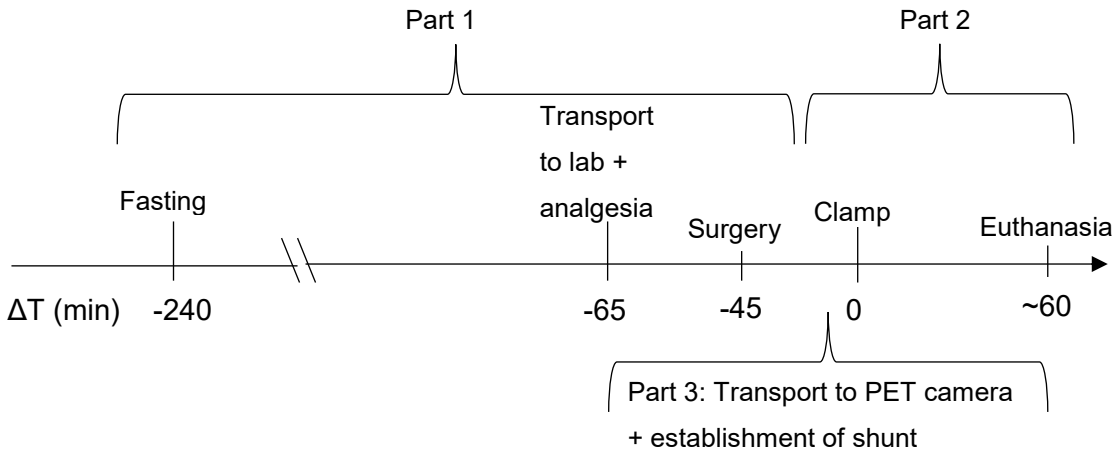

Figure 7 Study timeline. Parts 1 and 2 were conducted in the laboratory before part 3.

4.2 Experimental animals

All animal experiments of this study were approved by the State Provincial Office of Southern Finland (permission number ESAVI/4080/2019). Animal wellbeing complied with the ethical guidelines of the International Council of Laboratory Animal Science (ICLAS). All procedures were performed under terminal inhaled isoflurane-oxygen mixture anesthesia (Attane Vet 1000 mg/g, Piramal Healthcare UK Limited, Northumberland, United Kingdom). Eight to ten-week-old male Sprague-Dawley rats (n = 26; 345.1 ± 25.2 g) were provided by University of Turku Central Animal Laboratory in Turku, Finland. In practice, 8 rats were used for establishing the microsurgical technique and 18 rats were used for the clamp study, in which femoral vein-artery shunt system was employed for insulin and glucose infusion. Total of 12 animals divided into three different study groups (n = 4 per group) were included in the present clamp study.

Rats were housed in pairs or threes in ventilated cages. Animal housing room temperature was kept consistent at 21.0±1.1° C and humidity at 55±5 %. Light/dark cycle was 12 hours (dark period lasting from 1900h to 0700h). The rats were fed standard soy-free chow (RM3 soya-free, 801710, Special Diets Service, Essex, UK). The food and water were available *ab libitum*. The rats were fasted for 4 hours prior to each clamp procedure.

4.3 Study methods

4.3.1 Surgical Catheterization of Arterial and Venous Circulation

On the study date, the experimental animal was weighed and 0.05 mg/kg of buprenorphine (Temgesic, Reckitt Benckiser Healthcare (UK) Limited, Hull, United Kingdom) was injected subcutaneously. Anesthesia was induced 30 minutes after injection using isoflurane vaporized in oxygen. The animal was operated on a heating pad in order to maintain the body temperature.

The animal was prepared by removing hair from the surgical site (groin area) and secured to the surgical surface by taping the hind legs and the surgical site was disinfected with 70% ethanol. Sufficient level of anesthesia (2-2.5% isoflurane/700 ml oxygen) was ensured by checking for the presence of foot reflexes. An incision was made near the groin area on the left hind leg, parallel to the femoral vessels.

The proximal part of femoral vessels was exposed by blunt dissecting. The connective tissue was gently teased off from the vessels and the nerve isolated from the artery. Two approximately 15 cm long 6/0 non-absorbable silk suture threads (Nonabsorbable Braided Sil Suture, size: 6/0, item no: 18020-60, Fine Science Tools Inc., North Vancouver, B.C., Canada) were slid under the vein. One was used to close the vein just above the epigastric vessels with double sutures. The other was used to lift the vein from the underlying muscle and stop blood flow. A small cut was made in between the threads with micro spring scissors. PE-50 (20 cm length, 0.58 mm ID, 0.96 mm OD; Smiths Medical International Ltd, Kent, UK) tubing filled with 10 U/ml heparinized saline (9 mg/ml) was inserted into the vein and attached using the threads. The catheter patency was tested by pushing the heparinized saline into the vein with a syringe. If no sign of leakage and the catheter was cleared of blood, the syringe was replaced with a plug and the catheter fixed to place. The same procedure to insert the catheter was repeated for the artery (Figure 8).

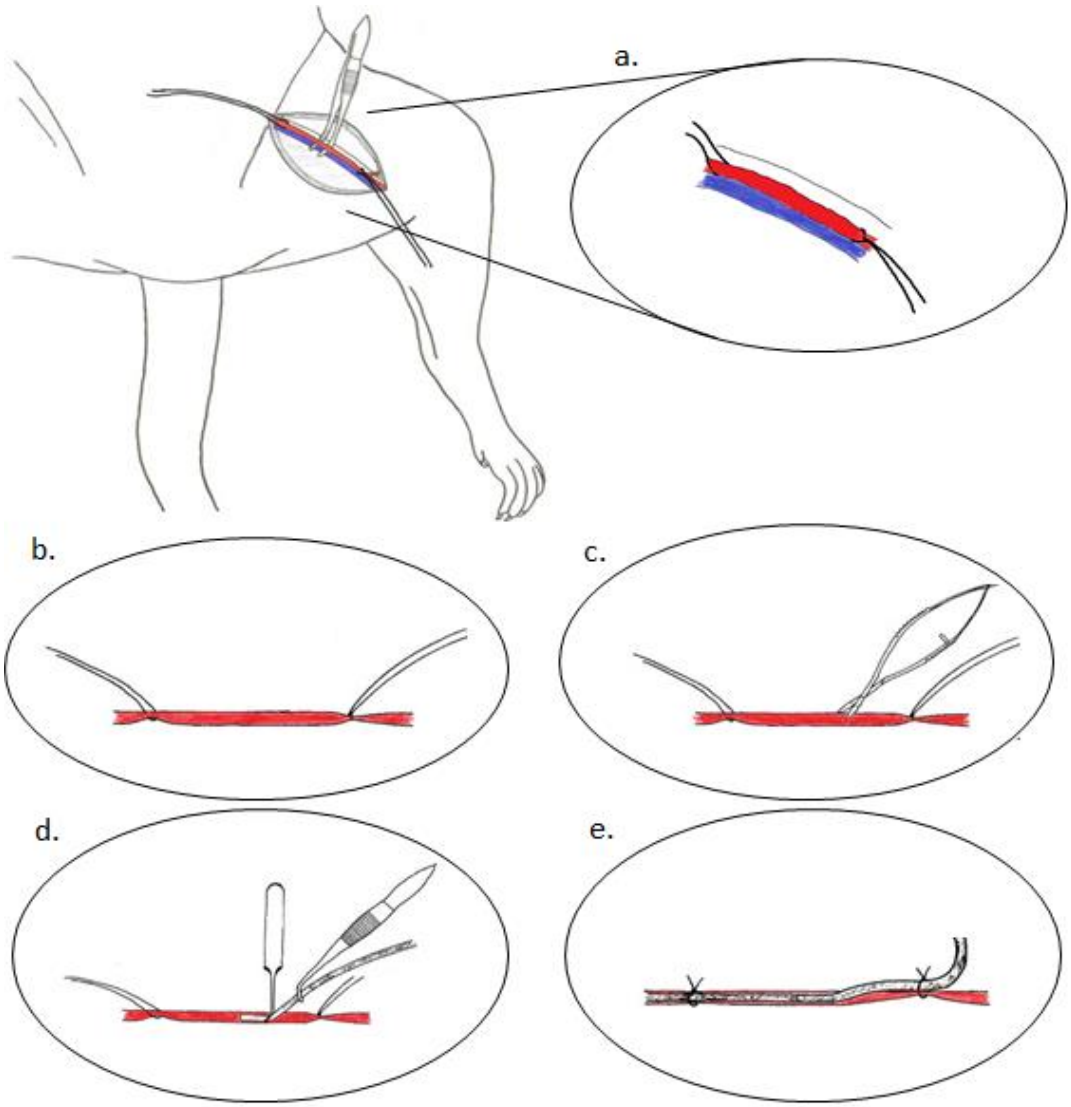

Figure 8 The catherization of femoral artery and vein. a. The artery (in red) was isolated from the vein (in blue) and nerve (in white). b. A suture thread was used to cut off the blood flow at the distal end of the exposed part of the artery. Another looped thread was used to lift the artery and prevent blood flow between the threads. c. A cut was made with micro-spring scissors close to the sutured end. d. The catheter tube was placed inside and slid past the looped thread at the proximal end of the exposed artery. e. Both threads were used to secure the catheter in place. The process for the catherization of the vein is identical.

4.3.2 Hyperinsulinemic-Euglycemic Clamp

Based on previous studies by other groups, two different insulin priming concentrations and two different constant rate concentrations were chosen to be tested. Su et al. (2014) used a priming insulin infusion of 50 mU/kg/min for the first two minutes of the clamp and a constant infusion of 5 mU/kg/min thereafter. Lapa et al. (2017) primed with 240 mU/kg/min insulin infusion for 20 minutes and used a constant infusion of 12 mU/kg/min thereafter. The order of animals undergoing the study was chosen at random to prevent showing favoritism to any of the groups. Insulin and glucose infusions were administered

using two syringe drivers (Braintree Scientific Inc., model no. BS-300) where 10 ml syringes were attached to the femoral vein catheter by connection tubing. The hyperinsulinemic euglycemic clamp was initiated by a 3-minute insulin priming at infusion rate of 120 or 50 mU/kg/min. After 3 min priming, the insulin infusion was decreased to a constant rate of 12 or 5 mU/kg/min and simultaneous 20 % glucose infusion was started at variable rate as necessary to maintain euglycemia (blood glucose 4.0-6.0 mmol/l; target level 5.0 mmol/l). Blood glucose concentrations were determined at least every 5 minutes from the lateral tail vein with Accu-Chek Aviva Nano portable glucometer (Roche Diagnostics, USA). The time to reach steady state in the target region was recorded. Steady state was defined as 10 minutes of consecutive blood glucose measurements within 1.0 mmol/l. The euglycemia was maintained for prolonged time in order to examine the possible challenges to maintain the steady-state blood glucose value in future *in vivo* imaging studies with radioisotope-labelled glucose. The different clamp study group conditions are presented in Table 2.

Table 1 Initial conditions for the clamp study.

Group	Insulin priming rate (mU/kg/min)	Constant insulin infusion rate (mU/kg/min)
1	120	12
2	50	12
3	120	3
4	50	3

Based on preliminary results, three of the aforementioned study groups were discarded and the most promising study group was chosen for optimization. Stepped priming was introduced to the design for priming. The steady state infusion rate for all groups was 12 mU/kg/min. The groups were studied mainly in alphabetical order. The final study group conditions for insulin priming are presented in Table 3. Blood glucose readings as well as changes in glucose infusion rate with timepoints were recorded on a worksheet.

Table 2 Final study group conditions for insulin priming. Steady state priming was 12 mU/kg/min for all groups.

Group	Priming
A	120 mU/kg/min for 3 min
B	120 mU/kg/min for 3 min followed by 60 mU/kg/min for 2 min
C	120 mU/kg/min for 2 min followed by 60 mU/kg/min for 2 min

4.3.3 Set up for *in vivo* imaging with hyperinsulinemic euglycemic clamp

A shunt system was constructed to enable online measurement of blood radioactivity at the Small Animal Imaging Unit of Turku PET Centre. The shunt was designed to be used when imaging rats with Inveon Multimodality PET/CT device (Siemens Medical Solutions, Knoxville, TN, USA). The shunt system enables steady arterial blood circulation at controlled flowrate via shunt pump ISMATEC® model REGLO Digital MS-2/12 (Cole-Parmer GmbH, Wertheim, Germany) and online blood radioactivity measurement with a coincidence detector Swisstrace Twilight II (Swisstrace GmbH, Menzingen, Switzerland. The components to create the shunt with necessary inlets and outlets are listed in Table 4.

The created tubing of the shunt system was connected to the arterial and venal catheter tubes. The outlet was sealed using a 18G needle with a cap to create a plug for sampling and the inlets were sealed with 18G cannulas (Vasofix® Braunüle®, B. Braun Melsungen AG, Melsungen, Germany) for easy administration of substances. A schematic illustration of the shunt system is presented in Figure 9.

Table 3 Components used to create the shunt tubing.

Component	Inner diameter (mm)	Supplier
Tygon ST R-3607 silicone tubing	1.52	IDEX Health & Science GmbH, Werthweim, Germany
Silicone Peroxide tubing	0.76	Cole-Parmer GmbH, Wertheim-Mondfeld, Germany
T-connector	1.6/1.6/1.6	Cole-Parmer GmbH, Wertheim-Mondfeld, Germany
Reducer	1.5/2.5	Cole-Parmer GmbH, Wertheim-Mondfeld, Germany

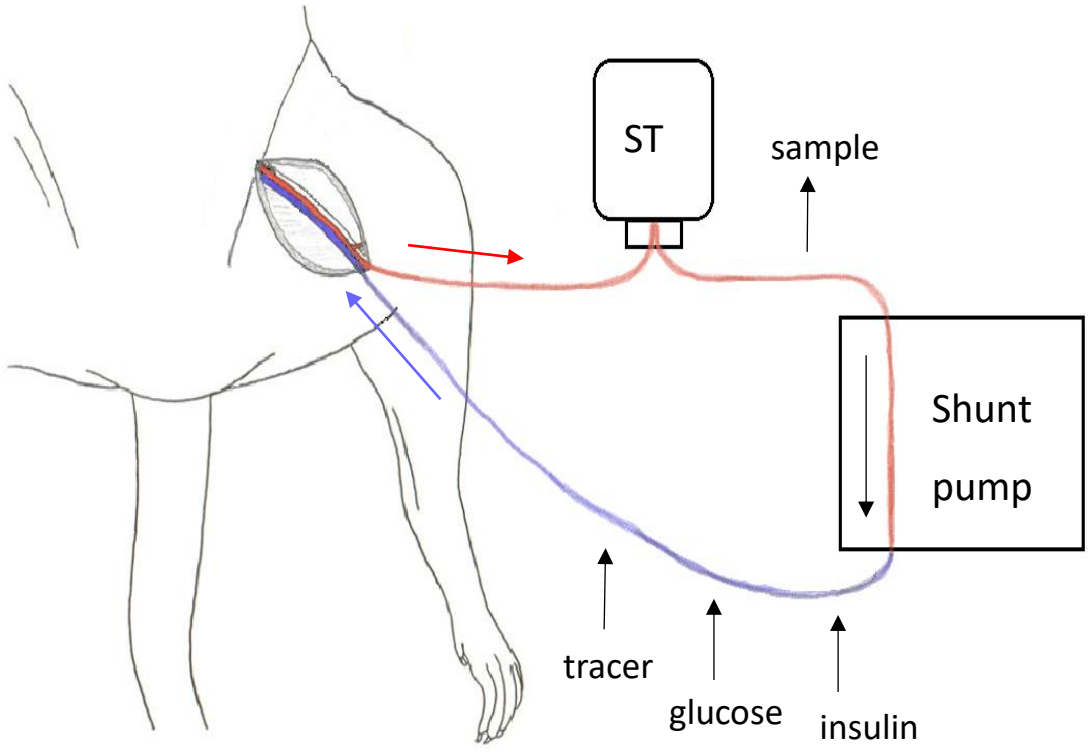

Figure 9. A schematic illustration of the shunt system for the insulin clamp. *ST*, Swisstrace twilite

4.3.4 Calculations and statistical analyses

Descriptive statistics, i.e. time to reach the euglycemic steady state in the clamp, weight of the animals, blood glucose values and M-values are presented as arithmetic means with standard deviations.

As the sample size per group is small and normal distribution cannot be assumed, the differences between study groups were examined with Kruskal-Wallis test, followed by Dunn's multiple comparison. The statistical significance level was set at 0.05. The statistical analyses were performed, and graphs drawn using GraphPad Prism v. 5.01 (GraphPad Software, San Diego, CA, USA) and Microsoft Excel v. 18.2008.12711.0 (Microsoft Corporation, Redmond, WA, USA)

5. Results

5.1 Surgical Catheterization of Arterial and Venous Circulation

All eight animals were successfully catheterized. The average duration of the surgery from the initiation of anesthesia to completion was 40 minutes. The reason for failure in microsurgery later in the study was puncturing the femoral vein with the cannula.

5.2 Hyperinsulinemic euglycemic clamp

Unfortunately, 5 experimental rats were discarded from the final results due to the failure in microsurgery or clamp, and one experimental rat died during the procedure. The initial testes insulin infusion rates had to be discarded as ineffective after five study subjects. Three of these individuals were removed from the study along with the study group. The individuals removed belonged to study groups 2 (n=2) and 4 (n=1). None of these three individuals had reached the steady state in the euglycemic area after 70 minutes of clamping. Three new insulin infusion rates were introduced for further examination in main rat groups of A, B, and C (Table 3). Descriptive results of the main rat groups (n=4 per group) for the clamp procedure are summarized in Table 5.

Table 4 Results per clamp study group. Results are presented as mean ± SD (n=4 per group).

	Weight (g)	Fasting blood glucose (mmol/L)	Postoperative blood glucose (mmol/L)	Time to reach steady state (min)	Blood glucose during clamp (mmol/l)	M-value (mg/min/kg)
Group A (ID1,3,5,8)	341.9±40.9	9.3±0.5	9.9±1.3	47.5±10.4	5.3±0.2	17.5±7.0
Group B (ID7,10,12,14)	344.5±28.3	8.1±0.7	8.3±0.6	41.3±6.3	5.3±0.3	19.5±3.8
Group C (ID15,16,17,18)	351.3±18.4	8.5±1.1	8.4±0.4	26.3±2.5	5.0±0.6	19.3±6.3

The most efficient clamping time was achieved with the conditions of study group C. In group A the blood glucose level initially started to decrease rapidly, but soon after priming was over, slowed significantly. In group B, the decline of blood glucose level was so rapid that in three out of four individuals the blood glucose dropped below the target area

before the effect of insulin could be reversed with external glucose. Blood glucose concentrations against time are presented in Figure 10.

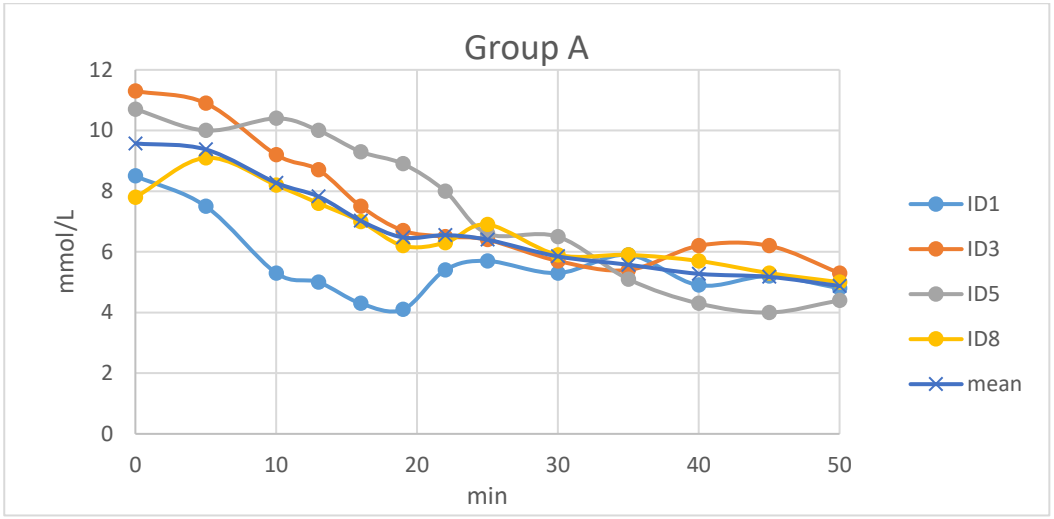

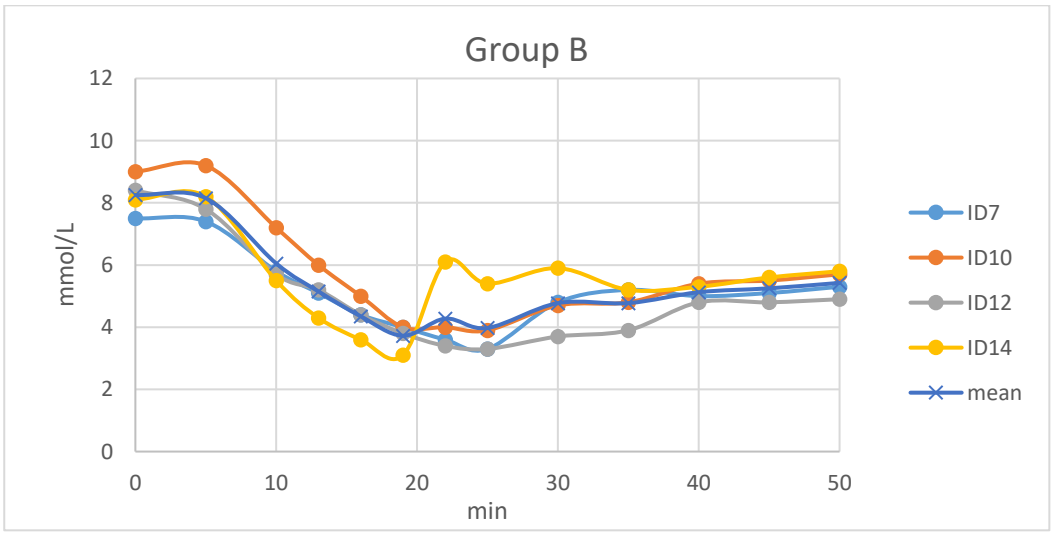

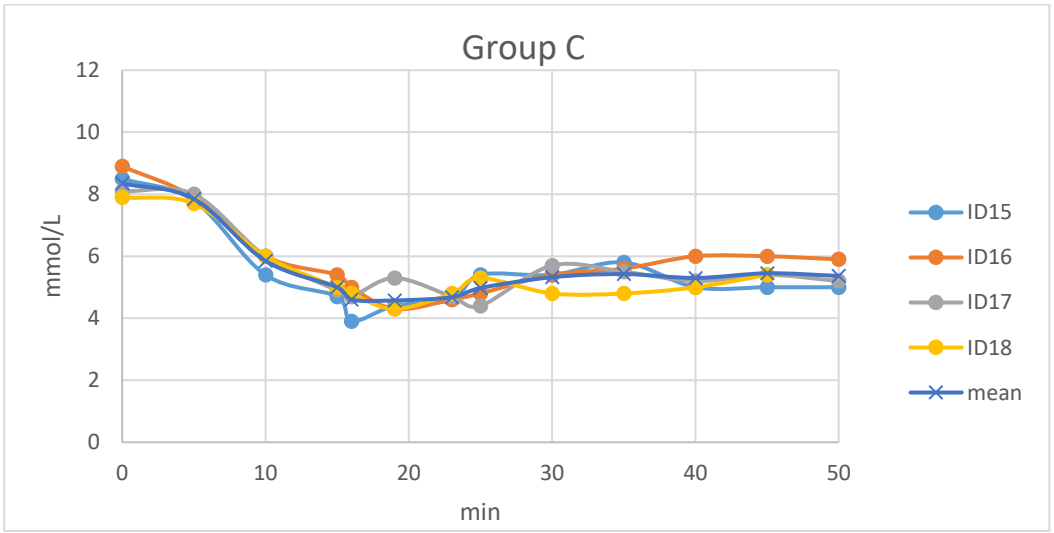

Figure 10 Blood glucose concentrations during clamp in groups A, B and C.

When comparing the clamping times, the Kruskal–Wallis test gives statistic $H = 7.868$, which is greater than the tabulated critical value of 5.692 for the significance level $\alpha = 0.05$. Thus, there is statistically significant difference between two or more insulin infusion conditions. Pairwise comparison with Dunn's multiple comparisons test revealed that there is statistically significant difference between groups A and C ($p < 0.05$), but not A and B or B and C ($p > 0.05$).

Comparisons between the rest of the variables presented in Table 5, i.e. the weight of the animal or the blood glucose during clamp, proved no differences between the study groups.

5.3 Shunt system for blood radioactivity measuring

The final layout of the shunt is presented in Figure 11. The length of the catheters inserted with surgery was increased to 35 cm to accommodate the needed length to establish flow through the Swisstrace Twilite cassette and the distance between the PET camera and clamp equipment. The cannula tubing was directly connected to the 0.76 mm ID silicone tubing, which acted as an adapter between the 1.52 mm ID pump tubing and catheter tubing. One outlet was placed after the Swisstrace detector for blood sampling, and three inlets were placed after the shunt pump for administration of glucose, insulin, and the radiotracer. The total volume of the shunt system is approximately 700 µL.

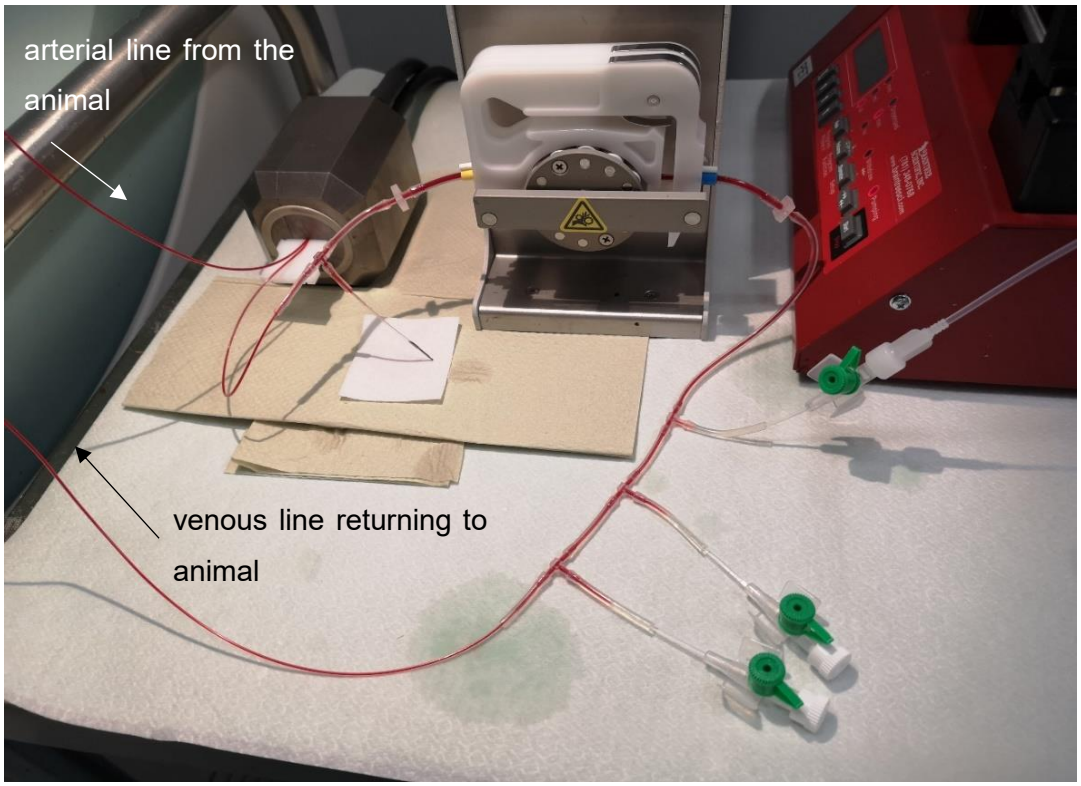

Figure 11 The shunt system at the PET camera. The shunt goes through the Swisstrace Twilite cassette, after which is the blood sampling point. The shunt pump prevents any backflow from the inlets, i.e. cannulas for insulin, glucose, and tracer to the sampling point. Insulin infusion syringe on the syringe drive connects to the cannula through connection tubing.

6. Discussion

6.1 Hyperinsulinemic euglycemic clamp

This thesis work aimed to develop a protocol for measuring tissue specific glucose uptake *in vivo* in the Sprague Dawley laboratory rat strain using hyperinsulinemic euglycemic clamp simultaneously with [^{18}F]FDG PET imaging. We compared three different insulin infusion conditions to determine the most time-efficient clamping conditions.

The shortest time to reach steady state in the clamp was achieved with insulin priming conditions of 120 mU/kg/min for 2 min followed by 60 mU/kg/min for 2 min (study condition C). The statistical calculations revealed that there was a significant difference between study condition A (priming at 120 mU/kg/min for 3 minutes) and study condition C, but not between study condition B (priming at 120 mU/kg/min for 3 minutes followed by 60 mU/kg/min for 2 min) and condition C. This might be due to the small number of animals per study group.

The mean GIRs or M-values for the study conditions A, B, and C were 17.5±7.0, 19.5±3.8, and 19.3±6.3 mg/kg/min, respectively. No significant difference was found between groups as was expected, assuming the study subject pool was homogenous and constant insulin infusion identical among groups. It has been shown that within normal range of plasma insulin and blood glucose of 2.8-9.2 mmol/L the insulin mediated glucose uptake is quite linear (Chan et al., 2010). If the GIRs from clamps performed on conscious unrestrained animals in Table 1 (Kraegen et al., 1983; James, Jenkins and Kraegen, 1985) are plotted against the insulin infusion rate, they seem to have linear correlation, albeit there being only three data points. If estimated based on that correlation, the mean M-value for this study pool should have been approximately 26 mg/kg/min. Estimation based on the three anesthetized previous studies presented in Table 1 (Spring-Robinson et al., 2009; Su et al., 2014; Lapa et al., 2017) would land on 13 mg/kg/min. The values attained in this study lie in between these two estimates derived from a small sampling of literature. The rat strains used in some of the presented previous studies differ from the strain used for this thesis, and also environmental variables probably vary between studies, making comparing values difficult.

Challenges in the clamp method are the environmental variables, mainly temperature, and anesthesia. The insulin clamp as such could be performed on conscious, chronically cannulated unrestrained animals (Kraegen et al., 1983; James, Jenkins and Kraegen, 1985), but the surgery for catheterization and PET imaging studies require sedation. Both clamp study and PET imaging are performed on awake individuals in clinical practice,

which could complicate comparing results with preclinical findings gathered under anesthesia. Isoflurane is known to elevate blood glucose level by inhibiting endogenous insulin production, but it should not affect the insulin sensitivity (Albrecht et al., 2014; Tanaka et al., 2009; Zuurbier et al., 2008). The clamp method does not rely on the body's ability to produce insulin but rather the insulin sensitivity. Therefore, it is presumed that should the anesthesia be kept at a constant level, it should not affect the results beyond the point, where the collected data becomes futile. In fact, to achieve the same effect of suppressing endogenous insulin production, somatostatin has been used in previous animal studies. (Farmer et al., 2015; Muniyappa et al., 2009)

Temperature affects glucose metabolism, and especially hypothermia is harmful for normal glucose uptake and the general well-being of the animal. In this study all the procedures were performed on a heating pad, but no record of core body temperature was kept. The heating conditions, i.e. the temperature of the heating pad, length of procedure, were similar for all the animals, so no great differences in the core temperatures are suspected.

6.2 Surgical catherization

The surgical catheterization of the femoral artery and vein is a laborious procedure requiring precision but showed to possess a steep learning curve and good success rate. Presumably the most fragile point of the surgery is inserting the venous cannula, as the tip of the cannula is prone to puncture the vein.

6.3 Set up for *in vivo* imaging

Previously, quantitative dynamic PET studies have been problematic to perform with small animals, as they require frequent manual blood sampling with substantially large blood volume to attain the blood activity curve, which means a great blood loss for the animal. This has made it virtually impossible to perform reliable quantitative kinetic analysis on mice due to their small size. Instead, rat is more attractive choice for quantitative PET studies due to its larger body size and blood volume capacity. Further, challenges in manual blood sampling can be overcome using automated blood samplers like the Swisstrace Twilite, where blood activity can be measured automatically while it circulates in a closed system. The system also contributes to work safety, as staff is no longer required to draw and handle radioactive blood. The volume outside the body should always be kept as small as possible to avoid hampering with the animal wellbeing.

The shunt system with automated blood sampler does not only serve the [^{18}F]FDG PET imaging protocols, but enables the AIF acquisition needed for quantitative kinetic

analysis for other tracer studies as well. Challenges in the shunt include blood clotting inside the tubing, which can be prevented with heparinized saline flushing and external heating of the tubing.

6.4 Study limitations

The small number of animals limited the significance of the statistics. The animal core temperature should have been recorded in order to detect any changes, that might affect the glucose uptake. The study design may create bias towards the last study group (study group C), as the researcher's familiarity with the catheterization and clamp procedure increased. This could have been avoided with a randomized study design.

In future clamp studies it is crucial to record the body temperature to detect possible changes and further normalize clamp data with individual temperature values.

6.5 Future prospects

The clamp protocol created in this study may be applied with slight modifications to accommodate for different rat strains with adjusted insulin infusion conditions specific for each strain. The protocol could also be miniaturized to suit mice with special tubing.

The site of cannulation could be switched to tail to make the procedure less invasive, like Guo and Zhou (2003) suggest. This would make post-operative care less tedious and shorten recovery time, making the clamp also more appealing to be used in longitudinal study designs.

7. Conclusions

This study created a protocol for hyperinsulinemic euglycemic clamp for rats that could be used simultaneously with *in vivo* [^{18}F]FDG PET imaging. For future studies, differences between rat strains might call for case-specific adjustments, but well-established ground knowledge shall lower the threshold for future studies involving the method.

Specific conclusions of the subobjectives:

I. The comparison of different insulin infusion rates showed, that using a two-stepped insulin priming of 120 mU/kg/min insulin infusion for 2 minutes followed by 60 mU/kg/min for 2 minutes and continuing with a constant infusion of 12 mU/kg/min, resulted in the shortest time to achieve “steady state” in the clamp experiment among the conditions being tested. A typical dropping pattern for blood glucose level observer and enabled the creation of a standardized work sheet templates to monitor different parameters during the clamp study.

II. The clamp study was successfully combined with dynamic *in vivo* [^{18}F]FDG PET imaging by using an external shunt system and an automated blood sampler Swisstrace Twilite II for blood activity measurement. The shunt system enables data collection for quantitative dynamic PET analysis also with other tracers.

Acknowledgements

Firstly, I want to thank my supervisor Jarna Hannukainen and the CROSSYS research team for providing me with this opportunity to work with state of the art methodology on a subject I am passionate about.

I want to thank Adjunct Professor Merja Haaparanta-Solin and the personnel of the PET project at Medicity Research Laboratory at University of Turku for providing me with the necessary tools and knowledge to guide me through my project. You made me feel welcome at the laboratory and have been the greatest joy to be around even on the toughest days.

I want to thank my professors and teachers at the Biomedical Imaging master's programme, whom, with their own passion, enthusiasm, and knowledge convinced me that I, too, wanted to be an expert in this field of science.

I want to thank my husband for supporting me all along and making me coffee for the long nights of writing.

Lastly but not least, I want to thank my other supervisor Jatta Helin (née Takkinen) who with her own example and some tough love inspired me to grow so much as a scientist. I still have a long way to go, but I have an excellent role model to guide my way.

References

Albrecht, M., Henke, J., Tacke, S., Markert, M. and Guth, B., 2014. Effects of isoflurane, ketamine-xylazine and a combination of medetomidine, midazolam and fentanyl on physiological variables continuously measured by telemetry in Wistar rats. *BMC Veterinary Research*, 10(1).

Alf, M., Wyss, M., Buck, A., Weber, B., Schibli, R. and Krämer, S., 2012. Quantification of Brain Glucose Metabolism by 18F-FDG PET with Real-Time Arterial and Image-Derived Input Function in Mice. *Journal of Nuclear Medicine*, 54(1), pp.132-138.

Almgren, P., Lehtovirta, M., Isomaa, B., Sarelin, L., Taskinen, M., Lyssenko, V., Tuomi, T. and Groop, L., 2011. Heritability and familiality of type 2 diabetes and related quantitative traits in the Botnia Study. *Diabetologia*, 54(11), pp.2811-2819.

American Diabetes Association, 2015. 2. Classification and Diagnosis of Diabetes. *Diabetes Care*, 38(Supplement_1), pp.S8-S16.

Armario, A., Montero, J. and Balasch, J., 1986. Sensitivity of corticosterone and some metabolic variables to graded levels of low intensity stresses in adult male rats. *Physiology & Behavior*, 37(4), pp.559-561.

Aronoff, S., Berkowitz, K., Shreiner, B. and Want, L., 2004. Glucose Metabolism and Regulation: Beyond Insulin and Glucagon. *Diabetes Spectrum*, 17(3), pp.183-190.

Ayala, J., Bracy, D., McGuinness, O. and Wasserman, D. (2006). Considerations in the Design of Hyperinsulinemic-Euglycemic Clamps in the Conscious Mouse. *Diabetes*, 55(2), pp.390-397.

Benedé-Ubieto, R., Estévez-Vázquez, O., Ramadori, P., Cubero, F. and Nevzorova, Y., 2020. Guidelines and Considerations for Metabolic Tolerance Tests in Mice . *Diabetes, Metabolic Syndrome and Obesity: Targets and Therapy*, Volume 13, pp.439-450.

Bergman, R., Ider, Y., Bowden, C. and Cobelli, C., 1979. Quantitative estimation of insulin sensitivity. *American Journal of Physiology-Endocrinology and Metabolism*, 236(6), pp.E667-77.

Bosgraaf, C., Suchy, H., Harrison, C. and Toth, L., 2004. Diagnosis: Pica Secondary to Buprenorphine Administration. *Lab Animal*, 33(3), pp.22-23.

Boston, R., Stefanovski, D., Moate, P., Sumner, A., Watanabe, R. and Bergman, R., 2003. MINMOD Millennium: A Computer Program to Calculate Glucose Effectiveness

and Insulin Sensitivity from the Frequently Sampled Intravenous Glucose Tolerance Test. *Diabetes Technology & Therapeutics*, 5(6), pp.1003-1015.

Braune, A., Hofheinz, F., Bluth, T., Kiss, T., Wittenstein, J., Scharffenberg, M., Kotzerke, J. and Gama de Abreu, M., 2019. Comparison of Static and Dynamic 18F-FDG PET/CT for Quantification of Pulmonary Inflammation in Acute Lung Injury. *Journal of Nuclear Medicine*, 60(11), pp.1629-1634.

Chan, A., Heinemann, L., Anderson, S., Breton, M. and Kovatchev, B., 2010. Nonlinear Metabolic Effect of Insulin Across the Blood Glucose Range in Patients with Type 1 Diabetes Mellitus. *Journal of Diabetes Science and Technology*, 4(4), pp.873-881.

Cheng, S., Yeh, J. and Flood, P., 2008. Anesthesia Matters: Patients Anesthetized with Propofol Have Less Postoperative Pain than Those Anesthetized with Isoflurane. *Anesthesia & Analgesia*, 106(1), pp.264-269.

Dadson, P., Landini, L., Helmiö, M., Hannukainen, J., Immonen, H., Honka, M., Bucci, M., Savisto, N., Soinio, M., Salminen, P., Parkkola, R., Pihlajamäki, J., Iozzo, P., Ferrannini, E. and Nuutila, P., 2015. Effect of Bariatric Surgery on Adipose Tissue Glucose Metabolism in Different Depots in Patients With or Without Type 2 Diabetes. *Diabetes Care*, 39(2), pp. 292-299.

DeFronzo, R., Tobin, J. and Andres, R., 1979. Glucose clamp technique: a method for quantifying insulin secretion and resistance. *American Journal of Physiology-Endocrinology and Metabolism*, 237(3), p.E214-E223.

DeFronzo, R., 1992. Pathogenesis of Type 2 (non-insulin dependent) diabetes mellitus: a balanced overview. *Diabetologia*, [online] 35(4), pp.389-397. Available at: <https://link.springer.com/content/pdf/10.1007/BF00401208.pdf> [Accessed 27 July 2020].

DeFronzo, R. and Tripathy, D., 2009. Skeletal Muscle Insulin Resistance Is the Primary Defect in Type 2 Diabetes. *Diabetes Care*, 32(suppl_2), pp.S157-S163.

DeFronzo, R., 2015. *International textbook of diabetes mellitus*. 4th ed. Chichester: Wiley Blackwell, p.235.

Diehl, K., Hull, R., Morton, D., Pfister, R., Rabemampianina, Y., Smith, D., Vidal, J. and Vorstenbosch, C., 2001. A good practice guide to the administration of substances and removal of blood, including routes and volumes. *Journal of Applied Toxicology*, 21(1), pp.15-23.

Dobrakovová, M., Kvetňanský, R., Opršalová, Z. and Ježová, D., 1993. Specificity of the effect of repeated handling on sympathetic-adrenomedullary and pituitary-adrenocortical activity in rats. *Psychoneuroendocrinology*, 18(3), pp.163-174.

Einstein, F., Fishman, S., Muzumdar, R., Yang, X., Atzmon, G. and Barzilai, N., 2008. Accretion of visceral fat and hepatic insulin resistance in pregnant rats. *American Journal of Physiology-Endocrinology and Metabolism*, 294(2), pp.E451-E455.

Farmer, T., Jenkins, E., O'Brien, T., McCoy, G., Havlik, A., Nass, E., Nicholson, W., Printz, R. and Shiota, M., 2015. Comparison of the physiological relevance of systemic vs. portal insulin delivery to evaluate whole body glucose flux during an insulin clamp. *American Journal of Physiology-Endocrinology and Metabolism*, 308(3), pp.E206-E222.

Florez, J., Hirschhorn, J. and Altshuler, D., 2003. THE INHERITED BASIS OF DIABETES MELLITUS: Implications for the Genetic Analysis of Complex Traits. *Annual Review of Genomics and Human Genetics*, 4(1), pp.257-291.

Fueger, B., Czernin, J., Hildebrandt, I., Tran, C., S. Halpern, B., Stout, D., Phelps, M. and Weber, W., 2006. Impact of Animal Handling on the Results of 18F-FDG PET Studies in Mice. *Journal of Nuclear Medicine*, 47(6), pp.999-1006.

Fuggle, N., Shaw, S., Dennison, E. and Cooper, C., 2017. Sarcopenia. *Best Practice & Research Clinical Rheumatology*, 31(2), pp.218-242.

Fuhrman, G. and Fuhrman, F., 1965. Effect of temperature on metabolism of glucose in vitro. *Cryobiology*, 1(3), p.245.

Gauna, C., Uitterlinden, P., Kramer, P., Kiewiet, R., Janssen, J., Delhanty, P., van Aken, M., Ghigo, E., Hofland, L., Themmen, A. and van der Lely, A., 2007. Intravenous Glucose Administration in Fasting Rats Has Differential Effects on Acylated and Unacylated Ghrelin in the Portal and Systemic Circulation: A Comparison between Portal and Peripheral Concentrations in Anesthetized Rats. *Endocrinology*, 148(11), pp.5278-5287.

Golden, S., Brown, A., Cauley, J., Chin, M., Gary-Webb, T., Kim, C., Sosa, J., Sumner, A. and Anton, B., 2012. Health Disparities in Endocrine Disorders: Biological, Clinical, and Nonclinical Factors—An Endocrine Society Scientific Statement. *The Journal of Clinical Endocrinology & Metabolism*, 97(9), pp.E1579-E1639.

Guo, Z. and Zhou, L., 2003. Dual Tail Catheters for Infusion and Sampling in Rats as an Efficient Platform for Metabolic Experiments. *Lab Animal*, 32(2), pp.45-48.

Haj Mouhamed, D., Ezzaher, A., Neffati, F., Douki, W., Gaha, L. and Najjar, M., 2016. Effect of cigarette smoking on insulin resistance risk. *Annales de Cardiologie et d'Angéiologie,* 65(1), pp.21-25.

Hocking, S., Samocha-Bonet, D., Milner, K., Greenfield, J. and Chisholm, D., 2013. Adiposity and Insulin Resistance in Humans: The Role of the Different Tissue and Cellular Lipid Depots. *Endocrine Reviews*, 34(4), pp.463-500.

Hücking, K., Watanabe, R., Stefanovski, D. and Bergman, R., 2008. OGTT-derived Measures of Insulin Sensitivity Are Confounded by Factors Other Than Insulin Sensitivity Itself. *Obesity*, 16(8), pp.1938-1945.

International Diabetes Federation, 2019. *IDF Diabetes Atlas, 9th edn.* Brussels, Belgium. Available at: https://www.diabetesatlas.org

James, D., Jenkins, A. and Kraegen, E., 1985. Heterogeneity of insulin action in individual muscles in vivo: euglycemic clamp studies in rats. *American Journal of Physiology-Endocrinology and Metabolism*, 248(5), pp.E567-E574.

Kaiser, F., Peltzer, T., Kreissl, M., Higuchi, T. and Arias-Loza, P., 2013. Impaired myocardial 18F-FDG uptake correlates with reduced level of hexokinase II but not GLUT4 expression in a rat model of type 2 diabetes mellitus. *Journal of Nuclear Medicine*, 54(Supplement 2), p.24.

Kale, V., Joshi, G., Gohil, P. and Jain, M., 2009. Effect of fasting duration on clinical pathology results in Wistar rats. *Veterinary Clinical Pathology*, 38(3), pp.361-366.

Katz, A., Nambi, S., Mather, K., Baron, A., Follmann, D., Sullivan, G. and Quon, M., 2000. Quantitative Insulin Sensitivity Check Index: A Simple, Accurate Method for Assessing Insulin Sensitivity In Humans. *The Journal of Clinical Endocrinology & Metabolism*, 85(7), pp.2402-2410.

Keyes JW, Jr. 1995. SUV: Standard uptake or silly useless value?. *Journal of Nuclear Medicine,* 36(10), pp.1836-9.

Khroyan, T., Wu, J., Polgar, W., Cami-Kobeci, G., Fotaki, N., Husbands, S. and Toll, L., 2014. BU08073 a buprenorphine analogue with partial agonist activity at μ-receptorsin vitrobut long-lasting opioid antagonist activityin vivoin mice. *British Journal of Pharmacology*, 172(2), pp.668-680.

Kodama, K., Tojjar, D., Yamada, S., Toda, K., Patel, C. and Butte, A., 2013. Ethnic Differences in the Relationship Between Insulin Sensitivity and Insulin Response: A systematic review and meta-analysis. *Diabetes Care*, 36(6), pp.1789-1796.

Kraegen, E., James, D., Bennett, S. and Chisholm, D., 1983. In vivo insulin sensitivity in the rat determined by euglycemic clamp. *American Journal of Physiology-Endocrinology and Metabolism*, 245(1), pp.E1-E7.

Lapa, C., Arias-Loza, P., Hayakawa, N., Wakabayashi, H., Werner, R., Chen, X., Shinaji, T., Herrmann, K., Pelzer, T. and Higuchi, T. (2017). Whitening and Impaired Glucose Utilization of Brown Adipose Tissue in a Rat Model of Type 2 Diabetes Mellitus. *Scientific Reports*, 7(1).

Lee, S., Muniyappa, R., Yan, X., Chen, H., Yue, L., Hong, E., Kim, J. and Quon, M., 2008. Comparison between surrogate indexes of insulin sensitivity and resistance and hyperinsulinemic euglycemic clamp estimates in mice. *American Journal of Physiology-Endocrinology and Metabolism*, 294(2), pp.E261-E270.

Li, X., Leng, S. and Song, D., 2015. Link between type 2 diabetes and Alzheimer’s disease: from epidemiology to mechanism and treatment. *Clinical Interventions in Aging*, 10, p.549.

Lin, E. and Alavi, A., 2019. *PET and PET/CT*. 3rd ed. Thieme, p.12-15.

Lutfy, K. and Cowan, A., 2004. Buprenorphine: A Unique Drug with Complex Pharmacology. *Current Neuropharmacology*, 2(4), pp.395-402.

Lømo, T., Eken, T., Bekkestad Rein, E. and Njå, A., 2019. Body temperature control in rats by muscle tone during rest or sleep. *Acta Physiologica*, 228(2).

MacAskill, M., Walton, T., Williams, L., Morgan, T., Alcaide-Corral, C., Dweck, M., Gray, G., Newby, D., Lucatelli, C., Sutherland, A., Pimlott, S. and Tavares, A., 2019. Kinetic modelling and quantification bias in small animal PET studies with [18F]AB5186, a novel 18 kDa translocator protein radiotracer. *PLOS ONE*, 14(5), p.e0217515.

Matthews, D., Hosker, J., Rudenski, A., Naylor, B., Treacher, D. and Turner, R., 1985. Homeostasis model assessment: insulin resistance and β-cell function from fasting plasma glucose and insulin concentrations in man. *Diabetologia*, 28(7), pp.412-419.

Meigs, J., Cupples, L. and Wilson, P., 2000. Parental transmission of type 2 diabetes: the Framingham Offspring Study. *Diabetes*, 49(12), pp.2201-2207.

Morley, J., Vellas, B., Abellan van Kan, G., Anker, S., Bauer, J., Bernabei, R., Cesari, M., Chumlea, W., Doehner, W., Evans, J., Fried, L., Guralnik, J., Katz, P., Malmstrom, T., McCarter, R., Gutierrez Robledo, L., Rockwood, K., von Haehling, S., Vandewoude, M. and Walston, J., 2013. Frailty Consensus: A Call to Action. *Journal of the American Medical Directors Association*, 14(6), pp.392-397.

Muc, R., Saracen, A. and Grabska-Liberek, I. (2018). Associations of diabetic retinopathy with retinal neurodegeneration on the background of diabetes mellitus. Overview of recent medical studies with an assessment of the impact on healthcare systems. *Open Medicine*, 13(1), pp.130-136.

Muniyappa, R., Lee, S., Chen, H. and Quon, M., 2008. Current approaches for assessing insulin sensitivity and resistance in vivo: advantages, limitations, and appropriate usage. *American Journal of Physiology-Endocrinology and Metabolism*, 294(1), pp.E15-E26.

Muniyappa, R., Chen, H., Muzumdar, R., Einstein, F., Yan, X., Yue, L., Barzilai, N. and Quon, M., 2009. Comparison between surrogate indexes of insulin sensitivity/resistance and hyperinsulinemic euglycemic clamp estimates in rats. *American Journal of Physiology-Endocrinology and Metabolism*, 297(5), pp.E1023-E1029.

Nieuwenhuizen, Schuiling, Bonen, Paans, Vaalburg and Koiter, 1998. Glucose consumption by various tissues in pregnant rats: effects of a 6-day euglycaemic hyperinsulinaemic clamp. *Acta Physiologica Scandinavica*, 164(3), pp.325-334.

Nuutila, P., Knuuti, M., Maki, M., Laine, H., Ruotsalainen, U., Teras, M., Haaparanta, M., Solin, O. and Yki-Jarvinen, H., 1995. Gender and Insulin Sensitivity in the Heart and in Skeletal Muscles: Studies Using Positron Emission Tomography. *Diabetes*, 44(1), pp.31-36.

Pacini, G. and Bergman, R., 1986. MINMOD: a computer program to calculate insulin sensitivity and pancreatic responsivity from the frequently sampled intravenous glucose tolerance test. *Computer Methods and Programs in Biomedicine*, 23(2), pp.113-122.

Perseghin, G., Ghosh, S., Gerow, K. and Shulman, G., 1997. Metabolic Defects in Lean Nondiabetic Offspring of NIDDM Parents: A Cross-Sectional Study. *Diabetes*, 46(6), pp.1001-1009.

Phelps, M., Huang, S., Hoffman, E., Selin, C., Sokoloff, L. and Kuhl, D., 1979. Tomographic measurement of local cerebral glucose metabolic rate in humans with (F-18)2-fluoro-2-deoxy-D-glucose: Validation of method. *Annals of Neurology*, 6(5), pp.371-388.

Phelps, M., 2000. Positron emission tomography provides molecular imaging of biological processes.*Proceedings of the National Academy of Sciences*, 97(16), pp.9226-9233.

Poulsen, P., Ohm Kyvik, K., Vaag, A. and Beck-Nielsen, H., 1999. Heritability of Type II (non-insulin-dependent) diabetes mellitus and abnormal glucose tolerance - a population-based twin study.*Diabetologia*, 42(2), pp.139-145.

Ravindran, R., Devi, R., Samson, J. and Senthilvelan, M., 2005. Noise-Stress-Induced Brain Neurotransmitter Changes and the Effect of Ocimum sanctum (Linn) Treatment in Albino Rats. *Journal of Pharmacological Sciences*, 98(4), pp.354-360.

Riddy, D., Delerive, P., Summers, R., Sexton, P. and Langmead, C., 2017. G Protein–Coupled Receptors Targeting Insulin Resistance, Obesity, and Type 2 Diabetes Mellitus. *Pharmacological Reviews*, 70(1), pp.39-67.

Saha, P., 2016. *Basics of PET Imaging*. Cham: Springer International Publishing.

Sano, Y., Ito, S., Yoneda, M., Nagasawa, K., Matsuura, N., Yamada, Y., Uchinaka, A., Bando, Y., Murohara, T. and Nagata, K. (2016). Effects of various types of anesthesia on hemodynamics, cardiac function, and glucose and lipid metabolism in rats. *American Journal of Physiology-Heart and Circulatory Physiology*, 311(6), pp.H1360-H1366.

Schönfeld, P. and Reiser, G., 2013. Why does Brain Metabolism not Favor Burning of Fatty Acids to Provide Energy? - Reflections on Disadvantages of the Use of Free Fatty Acids as Fuel for Brain. *Journal of Cerebral Blood Flow & Metabolism*, [online] 33(10), pp.1493-1499. Available at: <https://www.ncbi.nlm.nih.gov/pmc/articles/PMC3790936/> [Accessed 27 July 2020].

Spring-Robinson, C., Chandramouli, V., Schumann, W., Faulhaber, P., Wang, Y., Wu, C., Ismail-Beigi, F. and Muzic, R., 2009. Uptake of 18F-Labeled 6-Fluoro-6-Deoxy-D-Glucose by Skeletal Muscle Is Responsive to Insulin Stimulation. *Journal of Nuclear Medicine*, 50(6), pp.912-919.

Srikanthan, P. and Karlamangla, A., 2011. Relative Muscle Mass Is Inversely Associated with Insulin Resistance and Prediabetes. Findings from The Third National Health and Nutrition Examination Survey. *The Journal of Clinical Endocrinology & Metabolism*, 96(9), pp.2898-2903.

Steffen, J., 1988. Glucose, glycogen, and insulin responses in the hypothermic rat. *Cryobiology*, 25(2), pp.94-101.

Su, K., Chandramouli, V., Ismail-Beigi, F. and Muzic, R. (2014). Dexamethasone-Induced Insulin Resistance: Kinetic Modeling Using Novel PET Radiopharmaceutical 6-Deoxy-6-[18F]fluoro-d-glucose. *Molecular Imaging and Biology*, 16(5), pp.710-720.

Suckow, M., Hankenson, F., Wilson, R. and Foley, P., 2019. *The laboratory rat*. 3rd ed. San Diego: Elsevier Science & Technology, p.364.

Szablewski, L., 2011. *Glucose Homeostasis And Insulin Resistance*. 1st ed. Sharjah: Bentham Science Publishers, pp.47-48.

Tam, C., Xie, W., Johnson, W., Cefalu, W., Redman, L. and Ravussin, E., 2012. Defining Insulin Resistance From Hyperinsulinemic-Euglycemic Clamps. *Diabetes Care*, 35(7), pp.1605-1610.

Tanaka, K., Kawano, T., Tomino, T., Kawano, H., Okada, T., Oshita, S., Takahashi, A. and Nakaya, Y., 2009. Mechanisms of Impaired Glucose Tolerance and Insulin Secretion during Isoflurane Anesthesia. *Anesthesiology*, 111(5), pp.1044-1051.

Wasserman, D., Ayala, J. and McGuinness, O. (2009). Lost in Translation. *Diabetes*, 58(9), pp.1947-1950.

WHO, 2020. *Obesity And Overweight*. [online] Who.int. Available at: <https://www.who.int/news-room/fact-sheets/detail/obesity-and-overweight> [Accessed 10 December 2020].

Zhang, K., Herzog, H., Mauler, J., Filss, C., Okell, T., Kops, E., Tellmann, L., Fischer, T., Brocke, B., Sturm, W., Coenen, H. and Shah, N., 2014. Comparison of Cerebral Blood Flow Acquired by Simultaneous [15O]Water Positron Emission Tomography and Arterial Spin Labeling Magnetic Resonance Imaging. *Journal of Cerebral Blood Flow & Metabolism*, 34(8), pp.1373-1380.

Zuurbier, C., Keijzers, P., Koeman, A., Van Wezel, H. and Hollmann, M. (2008). Anesthesia's Effects on Plasma Glucose and Insulin and Cardiac Hexokinase at Similar Hemodynamics and Without Major Surgical Stress in Fed Rats. *Anesthesia & Analgesia*, 106(1), pp.135-142.